Title

A NEUTRAL-BEAM DIAGNOSTIC FOR FAST CONFINED ALPHA PARTICLES IN A BURNING PLASMA: APPLICATION ON CIT

Authors

Schlachter, A.S.
Stearns, J.W.
Cooper, W.S.

Publication Date

1987-10-01

LBL-24235
UC-34A

Lawrence Berkeley Laboratory
UNIVERSITY OF CALIFORNIA

Accelerator & Fusion Research Division

A Neutral-Beam Diagnostic for Fast Confined Alpha Particles in a Burning Plasma: Application on CIT

A.S. Schlachter, J.W. Stearns,
and W.S. Cooper

October 1987

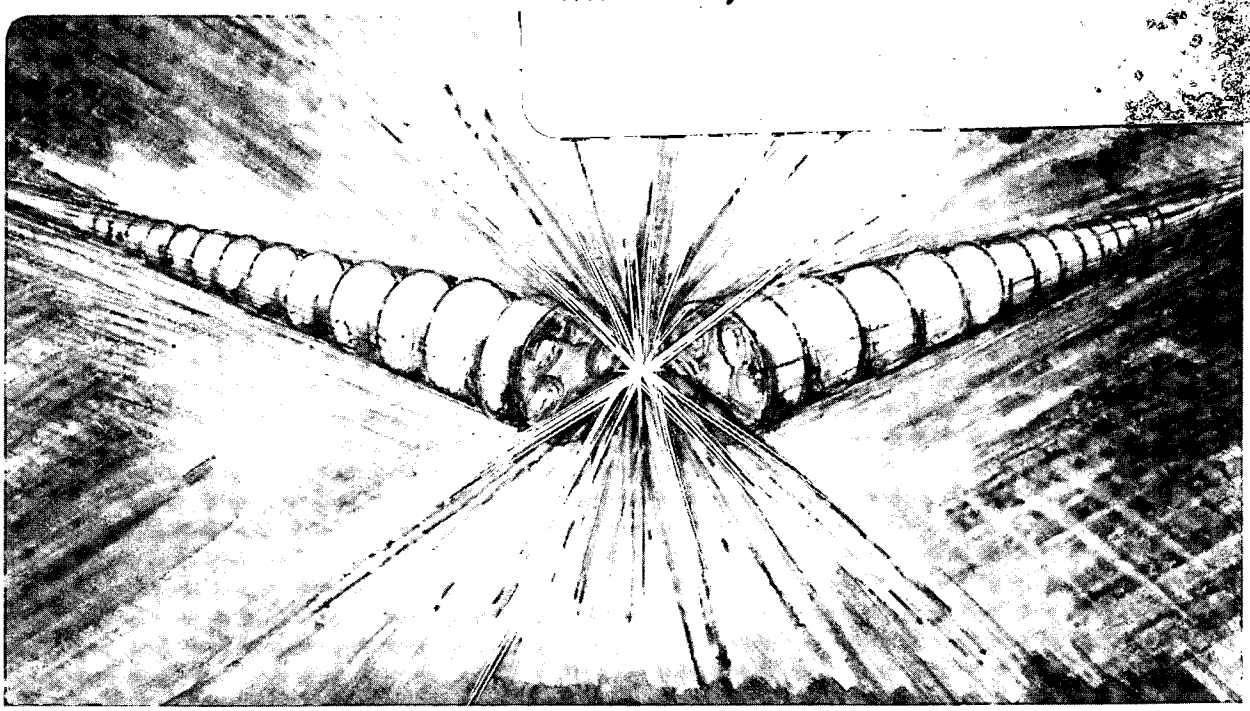

Prepared for the U.S. Department of Energy under Contract DE-AC03-76SF00098

DISCLAIMER

LBL-24235

A NEUTRAL-BEAM DIAGNOSTIC FOR FAST CONFINED ALPHA PARTICLES IN A BURNING PLASMA: APPLICATION ON CIT*

A. S. Schlachter, J. W. Stearns, and W. S. Cooper

Lawrence Berkeley Laboratory
University of California
Berkeley, CA 94720

October 28, l987

*Supported by U.S. DOE under Contract Number DE-AC03-76SF00098.

A NEUTRAL-BEAM DIAGNOSTIC FOR FAST CONFINED ALPHA PARTICLES IN A BURNING PLASMA: APPLICATION ON CIT

A. S. Schlachter, J. W. Stearns, and W. S. Cooper

Lawrence Berkeley Laboratory
University of California
Berkeley, CA 94720

October 28, 1987

Diagnostic methods for fast confined alpha particles are essential for a burning-plasma experiment. We review one- and two-electron-capture methods using energetic neutral beams, and provide quantitative estimates of signal level for a two-electron-capture method applicable to CIT. The best probe is a ground-state helium-atom beam because of its relatively good penetration into a CIT plasma and the large cross section for two-electron capture; it can be produced in useful quantities from HeH^+. We calculate a signal level of the order of 10^7 counts/s for 100 mA of accelerated HeH^+, which is sufficient to allow time-resolved measurements of the alpha-particle velocity distribution. Limited position information could be obtained for appropriate access port geometry. This diagnostic is feasible, and we recommend further research and development leading to implementation on CIT.

INTRODUCTION

Alpha particles (He^{++} ions) produced in the d-t fusion reaction

$$d + t \rightarrow He^{++}(3.5\ MeV) + n(14.1\ MeV) \qquad (1)$$

are born at an energy of 3.5 MeV, or 880 keV/u in the center of mass. Most are trapped in the magnetic field confining the plasma and slow down by interaction with plasma ions and electrons, thereby heating the plasma. The plasma is called "ignited" when the alpha particles produced by the d-t fusion reaction provide sufficient heat to the plasma to sustain the reaction, i.e., a "burning" plasma.

A new generation of tokamaks is being planned in which a primary objective is to achieve ignition. An essential diagnostic is measurement of the spatial, temporal, and velocity distribution of the fast alpha particles as they slow down, to ascertain whether they slow down classically or by some other energy-loss mechanism, and to answer questions concerning alpha-particle confinement and efficiency of alpha-particle heating.

Alpha particles will have a distribution of velocities as they slow down. Most of them will be confined by the magnetic field of the tokamak, while some will escape. The energy distribution of escaping alpha particles can be measured relatively easily; however, this does not characterize the confined alpha-particle distribution. Neutrons from the d-t reaction (1) will not be confined, but their spatial and energy distribution can be used to describe only the thermalization and confinement of the reactants. Measurement of the energy distribution of the alpha particles which are confined will be very useful in determining how well their energy is coupled to the bulk of the plasma. We address here methods of detecting fast confined alpha particles.

Development of a diagnostic method for fast confined alpha particles is difficult because of the high energy of the alpha particles and because of the minimal access to and large background emission from a burning-plasma reactor. Parameters for the current United States project, CIT (Compact Ignition Tokamak) include electron and ion densities of the order of 3.5 x 10^{14} cm^{-3}, electron and ion temperatures greater than 10 keV, alpha-particle density of 3 x 10^{13} cm^{-3}, and minor radius of 55 cm with an elongation of 2. CIT will be small and compact, with limited access for diagnostics. The burning plasma will generate a considerable flux of neutrons and photons, and neutron activation of materials will require remote-handling capability for materials and equipment located within the neutron shielding.

The topic of alpha-particle diagnostics and related atomic-physics issues has been recently reviewed by members of the Princeton Plasma Physics group (Post, Zweben, Grisham, and Fonck)[1-3], by Schumacher,[4] and by Schlachter and Cooper,[5] and alpha-particle effects were the topic by a recent workshop.[6] Background information is discussed in important articles by Post, Grisham, and co-workers at PPPL,[7,8] by partipants in the NYU workshop,[6] and in work from Nagoya.[9,10]

A variety of diagnostic methods has been proposed[6]; these methods include laser techniques (e.g., small-angle CO_2-laser Thomson scattering), microwave techniques (e.g., lower-hybrid-wave damping, ion-cyclotron emission), nuclear reactions (gamma-ray emission), pellet injection, and charge transfer with an energetic beam of atoms injected into the plasma.

The neutral-beam-based methods considered for a diagnostic for fast confined alpha particles are

a) single-electron capture by the fast alpha particles, He^{++}, from an energetic neutral beam injected into the plasma to serve as a charge-transfer target (charge-exchange recombination spectroscopy, or CHERS), leading to emission of a photon from excited states of He^{+}:

$$He^{++} + X \rightarrow He^{+*}(n\ell) + [X^{+}] \rightarrow He^{+} + h\nu + [X^{+}]; \quad (2)$$

(b) two-electron capture by the fast alpha particles, He^{++}, from an energetic neutral beam injected into the plasma, creating a fast He atom which, being neutral, can escape the confining magnetic field:

$$He^{++} + X \rightarrow He^{0} + [X^{++}]; \text{ and} \quad (3)$$

(c) nuclear methods, in which the alpha particle interacts with target nuclei which are introduced into the plasma, resulting in emission of a gamma ray.[11]

Non-beam-based methods for alpha-particle diagnostics have also been proposed, as well as diagnostics on the neutrons which are also emitted in the d-t reaction. Methods (a) and (b) have been discussed by Post et al.,[8] while an implementation of method (b) using a Li^{0} beam has been discussed by Grisham et al.[7] and, using a He^{0} beam, by Sasao and Sato.[9]

Methods (a) and (b) are shown schematically in Fig. 1 for possible candidates for the target beam: H^{0} for reaction (2) and He^{0} for reaction (3). Cross sections for reactions (2) and (3) are shown in Fig. 2. As Post et al. have discussed,[8] the cross sections for the reactions shown in Fig. 2 are small for high velocities, and thus the diagnostic method has velocity

selectivity, i.e., fast alpha particles interact essentially only with injected target atoms of about the same velocity (magnitude and direction). Varying the velocity of the injected target beam will allow measurement of the velocity distribution of the fast alpha particles.

We are concerned primarily with the feasibility of a neutral-beam diagnostic for fast confined alpha particles for CIT. The CIT parameters we have used are shown in Table I.

Table I. CIT Parameters

minor radius:	55 cm
elongation:	2
effective vertical path length	200 cm
n_i:	3.5×10^{14} cm^{-3}
n_e:	4.7×10^{14} cm^{-3}
Z_{eff}:	1.5 (carbon impurity)
vertical-access ports:	5-cm diameter, 5-m separation
n_α:	3×10^{13} cm^{-3}
$T_i = T_e$	10 keV

The geometry we have assumed is shown in Fig. 2.

Quantitative analysis is given for the 2-electron-capture method, which we find to be very promising.

DESCRIPTION OF SINGLE-ELECTRON CAPTURE TO FORM $He^+(n\ell)$ FOLLOWED BY PHOTON EMISSION (CHERS)

The method of single-electron capture by a fast confined alpha particle from a neutral atomic beam injected to serve as a charge-transfer target is a form of charge-exchange recombination spectroscopy (CHERS).[12] Most of the He^+ formed by electron capture will be in an excited state, $He^+(n\ell)$, where $n\ell$ refers to the quantum numbers of the state ($n>1$), and will therefore decay radiatively with emission of a photon from the He^+ spectrum, which can be detected outside the plasma. This approach has been described by Post et al.[8]

The neutral beam serving as a charge-transfer target must have a velocity close to that of the alpha particles to be detected in order to be useful, because the cross section for electron capture is appreciable only at small relative velocities. For example, Fig. 3 shows estimated cross sections for reaction 2 using a fast H^0 beam, which is presently being developed at LBL and elsewhere. The cross sections for $He^{2+} + H^0 \rightarrow He^+(n\ell)$ were estimated by comparing calculations by R. E. Olson[13] with measured cross sections for electron capture into all states of He^+ and into the $He^+(2s)$ state.[14] The accuracy of these estimated cross sections is, at best, a factor of 2, and could be considerably worse. Electron capture into the n=2 state predominates because the reaction is accidentally resonant for collision with a ground-state H^0 atom. The $He^+(n=2)$ state decays radiatively with the emission of a photon at 304 Å, well into the vacuum ultraviolet spectral region. The estimated cross section for formation of $He^+(n=3)$ shows a broad peak at higher energy than the cross section for formation of $He^+(n=2)$, and lower in magnitude by approximately a factor of ten. The estimated cross sections for formation of $He^+(n=4)$ and $He^+(n=5)$ are less by approximately another factor of

2 and 4, respectively, than the $He^+(n=3)$ cross section. The $He^+(n=3)$ level decays radiatively with the emission of a photon at 1640 Å, for which refractive optics are useable; the $He^+(n=4\rightarrow3)$ transition is in the visible (blue) spectral range at 4686 Å. These transitions are shown in Fig. 4. Note that the He^+ spectrum is the same as the H^0 spectrum, but with energies higher by a factor of 4; e.g., $He^+(4\rightarrow2)$ radiates at the same energy as $H^0(2\rightarrow1)$, which is Lyman-alpha for H atoms.

The photons radiated by $He^+(n\ell)$ will be Doppler-shifted because of the ion motion, and can thus be distinguished from radiation by slow He^+ ions which originate in the plasma along the line of sight. The photons are, however, emitted isotropically, and only a small fraction can be observed because of constraints imposed by limited access. Mirror and refractive optics can be used for $He^+(n=3\rightarrow2)$ radiation at 1640 Å; high-reflectivity multi-layer mirrors, which are fabricated at LBL and elsewhere, could be used for He^+ $(n=2\rightarrow1)$ radiation at 304 Å. The estimated spectral density for reasonable target-beam parameters in either case is estimated to be smaller than the bremsstrahlung background from the plasma, so that some signal-processing techniques will be needed.[16] The collecting mirror or lens will be exposed to an intense x-ray and neutron flux, so that radiation hardening will be a consideration in the design of a diagnostic system.

A beam of Li^0 or of a heavier species can be used as a charge-transfer target, giving a greater yield of $He^+(n=3)$ than would a beam of H^0. However, $He^+(n\ell)$ must radiate before being collisionally ionized, which limits the usefulness of $He^+(n)$ states with large values on n. Finally, the intense magnetic field of CIT (10 Tesla) will cause changes in state lifetimes, state populations, and decay rates, which must be taken into account.

DESCRIPTION OF TWO-ELECTRON CAPTURE TO FORM He^0

A fast alpha particle which captures 2 electrons from a target atom will become a fast neutral He atom, which has some likehood of traversing the plasma and, being neutral, will escape the confining magnetic field, where it can be reionized and energy analyzed, or otherwise detected. This approach has been described by Grisham et al,[7] who proposed the use of a fast Li^0 beam as the injected charge-transfer target. The cross section for 2-electron transfer[14,15,17-21] from various target atoms in collision with He^{++} is shown in Fig. 5; it is appreciable only at small relative velocities, hence the injected target beam must have a specific energy of the order of 880 keV/u to interact with alpha particles at their birth velocity.

Attenuation of the probe beam by ionizing collisions as it passes through the plasma is an important consideration, as is attenuation by ionization of the He^0 beam (neutralized alpha particles) traversing the plasma after the 2-electron-capture collision. The latter depends upon the state of the He^0 atoms; any state other than the ground $(1s)^2\ ^1S$ state is likely to be reionized in traversing the remaining plasma. However, it is likely that most of the He^0 beam will be in the ground state.[13] These topics are further discussed in later sections.

The choice of a probe beam for two-electron transfer is dictated partly by the requirement that the beam velocity be approximately equal to the birth velocity of the alpha particles. Thus use of a heavy atom would require a high energy to achieve the necessary velocity. Atomic hydrogen only has one electron, and is thus not a candidate. Potential candidates include He^0, Li^0, H_2^0, and other neutral species. As will be discussed in later sections, the penetration of Li^0 into a CIT plasma is poor. He^0 is an excellent candidate;

the well-known difficulty of producing fast ground-state He^0 is discussed below.

The fast atoms that exit the plasma (both neutralized alpha particles and un-reacted He atoms if He^0 is used as the probe beam) can be reionized and mass and energy analyzed, to discriminate against other ions and atoms which are emitted by the plasma. $^3He^0$ can be injected to distinguish neutralized alpha particles from injected helium atoms. Although the cross section for two-electron transfer is 1 to 2 orders of magnitude smaller than that for one-electron transfer to $He^+(n=2)$, essentially all the He^0 (neutralized alpha particles) which are not first reionized will exit the plasma in the direction of the incident target beam, compared with the isotropic emission of photons and the small solid angle of detection for the case of radiating $He^+(n=2)$, so a large signal can be obtained. Background is expected to be very small, as there are few other sources of fast He ions or atoms. (Although the d-d reaction does produce $^3He^{++}$, the cross section is small).

QUANTITATIVE DISCUSSION OF TWO-ELECTRON-CAPTURE DIAGNOSTIC

We have focussed our attention on the two-electron-transfer method to avoid two problems with the one-electron-transfer (CHERS) method: (1) having to look directly at the plasma, i.e., having a mirror exposed to the intense radiation flux from the plasma, and (2) having to separate the signal, consisting of photons emitted by $He^+(n\ell)$, from background, especially that due to bremsstrahlung. This is not to say that CHERS is not possible on CIT, only that it appears to be difficult. The CHERS method does have the considerable advantage, however, of being able to use a large port along the horizontal (narrow) dimension of the plasma: if the neutral beam is injected from the top or bottom through a small port, it needs to penetrate ~100 cm of plasma (not

200 cm, as in the two-electron-transfer case). The photon emission viewed at right angles to the target beam will give positional as well as energy information about the alpha-particle distribution. The other choice would be to inject the neutral beam through a large horizontal port, traversing only 50 cm of plasma, with a large improvement in beam penetration, but with photon viewing constrained to a small solid angle through small vertical port. We suggest that CHERS be studied further, along with study of an optical system that allows photon measurement at 304, 1640, or 4686 Å consistent with the level of radiation expected from the plasma.

Discussion of the two-electron-transfer method can be divided into parts: production of the neutral probe beam, penetration of this beam into the plasma, the two-electron charge-transfer process, survival of the fast He^0 (neutralized alpha particle) beam as it exits the plasma, and reionization and detection of the fast He^0. The fast He^0 beam exiting the plasma will be reionized in a gas or foil and detected after mass analysis; signal level rather than signal/noise will be of primary concern, as the detectors can be very well shielded, hence the noise level is expected to be low. This topic should be further studied.

TARGET BEAM SELECTION FOR TWO-ELECTRON-CAPTURE DIAGNOSTIC

We have assumed that the probe beam should be a neutral atomic or molecular beam of a relatively light species, because a specific energy of 880 keV/u (birth velocity of an alpha particle) corresponds to an unreasonably high energy for heavier species. The choices we have considered primarily are, He^0, H_2^0, Li^0, and other neutral atoms ranging in mass from C^0 to K^0. The cutoff at 39 amu is arbitrary; however, 880 keV/u requires an energy of 34 MeV

for K, and no compelling advantage is apparent for using a heavier (hence higher energy) species.

We have considered the possibility of using a singly charged heavy ion as a probe; however, the mass required to have a sufficiently large radius of curvature in the 10T field of CIT for a reduced energy of 880 keV/u is probably prohibitive. An ion of mass 74 (around As) or greater would be required for a radius of curvature greater than 100 cm, which corresponds to an energy of at least 65 MeV.

An intense energetic beam of neutral atoms or molecules can be produced by starting with a beam of ions from a suitable ion source. The beam is accelerated to a specific energy of the order of 880 keV/u, and then neutralized. Energetic beams of most species can be efficiently produced by neutralization of negative ions, e.g., energetic H^0 and Li^0 are be produced from H^- and Li^-. However, this is not the case for several species, which either do not exist as a negative ion (e.g., N^- does not seem to exist, and H_2^- and H_3^- do not exist), or, in the case of He^0, a metastable (rather than ground) state of He^0 is the primary product of neutralization of He^- in a gas. Molecular neutrals can be produced from positive molecular ions, e.g., a beam of H_2^0 can be produced by breakup of H_3^+, and a beam of (presumably ground-state) He^0 can be produced by breakup of HeH^+ or He_2^+ (or perhaps He_2^-). These are not the only possibilities; one can imagine various long-chain molecular ions which can be dissociated in a gas target to produce useful neutral particles. He-containing molecular ions other than HeH^+ might be more efficient for producing He^0; this topic should be further explored.

The problem of producing a beam of fast ground-state He atoms is now well known.[22] He^- exists in the metastable $(1s2s2p)\,^4P_J$ quartet state, in which all three electron spins are aligned. Neutralization by a collision in a gas

leads primarily to the $(1s2s)^3S$ metastable state of He^0, which, being only 4 eV from ionization, would have very poor penetration into a CIT plasma. Sasao and Sato[9] have proposed letting He^- autoionize (the J = 1/2 and 3/2 states have lifetimes of the order of 20 μs); a He^- beam at 880 keV/u (1.3×10^9 cm/s) would travel 260 m in one e-folding length, which might be too long for reasonable application.

We have made estimates of the formation of H_2^0 from breakup of H_3^+ and of He^0 from breakup of HeH^+ at an energy giving the product (H_2^0 or He^0) with a specific energy in the range 400 to 1000 keV/u; we used cross sections[23,24] for the relevant processes which are either known or can be estimated by extrapolation. The fraction of neutral products does not change rapidly with energy over this range. We have calculated the fraction of He^0 produced by breakup of 5-MeV HeH^+ in H_2, yielding 1 MeV/u He^0; charge-state fractions as a function of target thickness are shown in Fig. 6. An optimal fraction of 3% is obtained. H_2 production for 3-MeV H_3^+ in H_2 is shown in Fig. 7; the yield of 1-MeV/u H_2^0 is 4%. Although these yields are relatively small, the advantage is that positive ions are accelerated, which can be produced in copious quantities. Results are shown in both cases for an H_2 target, as this choice gives the best results of targets studied to date; additional targets should be considered.

We have experimentally tested the possibility of producing large fluxes of HeH^+ by running a mixture of He and H_2 in a volume-production ion source used for research on production of intense H^- beams. The preliminary result,[25] which we have not optimized, is that about 10% of the positive-ion output of this source is HeH^+. We expect to produce about 25 mA/cm^2 of HeH^+ (10% of a total current density of 250 mA/cm^2 at the source), which will yield approximately 1 mA/cm^2 of He^0, again referred to the plasma source.

An ion source can be optimized to produce H_3^+ by operation at high pressures. We expect to produce about 125 mA/cm^2 H_3^+ (250 mA/cm^2 total beam, of which 50% is H_3^+), which will yield approximately 4 mA/cm^2 of H_2^0 referred to the source.

We highly recommend further studies of novel methods of producing fast He^0 atoms, e.g., by dissociation of fast He_2^+ and even of He_2^-, neither of which has been studied. The ground-state fraction of He^0 should also be studied for each of these cases. Additionally, the brightness of a source to produce these molecular species should be measured.

Fast atoms of many species can be produced by neutralization of fast negative ions. The formation by charge transfer of negative ions of heavy species has been reviewed by Schlachter.[26] Furthermore, many negative ions, e.g., Li^-, can be formed in volume-production sources.[27] We expect that a current density of negative ions of 10 mA/cm^2 can be obtained,[28] and that the negative ions can be neutralized with 40-50% efficiency,[29] giving 5 mA/cm^2 (equivalent) atom flux density referred to the source.

The maximum neutral beam which can be injected into CIT through a 5-cm-diameter vertical port and exit through another 5-cm-diameter port 500 cm across the machine (Fig. 2) is determined by this port geometry, by the brightness of the ion source, by the accelerator optics, and by the current-handling capability of the accelerator. We have estimated in the preceeding paragraphs the equivalent current for various species which can be obtained. The brightness of high-intensity sources of H_3^+, HeH^+, and Li^+ is not known; we can, however, estimate brightness by analogy to H^+ ion sources; a well-designed ion source can produce a beam with 0.5 degree divergence at 100 keV. Brightness is conserved in acceleration in the absence of aberrations, and

the beam area multiplied by the square of the divergence angle scales inversely as the square of the velocity. The port geometry imposes an angle of 0.01 radian maximum (0.5^{o}). An accelerated beam which completely illuminates the entrance and exit ports described above, focussed to a waist in the center of CIT, will allow ions to be produced over a maximum source area of 600 cm^2 for a 3-MeV beam (600-keV/u HeH^+, 1-MeV/u H_3^+). An ion source with 600 cm^2 area could produce an equivalent atom current greater than 450 mA for He^o or 3000 mA for H_2^o or Li^o (see Table II). If we pick 100 mA as a reasonable ion current to be accelerated, we can calculate the appropriate area of the ion source, which will be considerably less than the 600 cm^2 allowed by the accelerator optics. We are thus not limited by ion-source performance but by the current-carrying capacity of the accelerator. Table II shows the estimated fast-atom flux which will obtained for 100 mA of accelerated ion current; X refers to any species for which negative ions can be produced.

Table II. Flux of fast atoms obtained for 100 mA of accelerated ion current

accelerated species	ion current density (mA/cm^2)	neutral yield	equivalent atom current density (mA/cm^2)	flux for 100 mA ion current (particles/s)
HeH^+	25	3% He^o	0.75	$2x10^{16}$
H_3^+	125	4% H_2^o	5	$2x10^{16}$
Li^-	10	50% Li^o	5	$3x10^{17}$
X^-	10	(30-50)% X^o	3-5	$(2-3)x10^{17}$

BEAM PENETRATION INTO A CIT PLASMA

A portion of a beam of neutral atoms or molecules injected into CIT will be ionized, and thus lost for diagnostic purposes. Fast helium atoms produced by two-electron capture (neutralized alpha particles) also will be subject to ionization along the path from their place of birth to their exit from the plasma. We have therefore determined effective cross sections for ionization of candidate neutral beams and neutralized alpha particles in a CIT plasma.

A comprehensive computer code (HEXNB) is available for calculating penetration of an H-atom beam into a plasma. A copy of this code, originally written at PPPL, was kindly furnished to us by Ed Synakowski and Roger Bengtson of the University of Texas; Doug Post of PPPL has supplied documentation,[30] and Chuck Boley, now at LLNL, provided a cosmetically improved version of the same code, called HEX, along with a fast code to calculate cross sections from fits to results of the HEX code, called FIT44.

We used these codes to calculate penetration of H^0 into a CIT plasma for a variety of conditions, concentrating primarily on a Z_{eff}=1.5 plasma containing carbon as the impurity, for H^0 energies in the range of 250-880 keV. The code optionally includes multi-step processes, i.e., excitation of H^0 to an excited state in one collision, followed by ionization from this state in a second collision. We also investigated the effect of assuming a parabolic or square-root of parabolic dependence for plasma density and temperature; the results for a slab and profiled plasma were similar to within several percent, hence all further calculations were done for a slab plasma.

We are not aware of the existence of a comprehensive beam penetration code valid at high energies (up to 1 MeV/u) for species other than H^0; a comprehensive code should include effects due to both plasma impurities and

multi-step processes. However, we can estimate beam penetration for species other than H^0, because at high energies, i.e., above a few hundred keV/u, ionization is due predominately to collisions of the fast atoms with the 10-keV H^+, D^+, or T^+ in the plasma; the electrons in a hot (10-keV) plasma are moving too fast to efficiently ionize the injected atoms. Cross sections[31-38] for ionization of various atoms and molecules by protons are generally known either experimentally or theoretically; examples are shown in Fig. 8. In some cases, where they are not known, the cross sections can be approximated by electron-ionization cross sections, because at high velocities, the cross section for ionization by protons and electrons is the same at the same velocity. We can therefore obtain an approximate ionization cross section by using the proton (or electron at the same velocity) ionization cross section. The effective beam-ionizing cross section in a plasma will be underestimated due to neglect of additional processes: (1) ionization by the electrons in the plasma (a small effect at beam energies of interest); (2) ionization by impurities in a $Z_{eff} = 1.5$ plasma, which has a larger effect; and (3) enhanced ionization due to multistep processes, which increases in importance for high beam energies and high Z_{eff}.[39] In order to estimate the effect on beam penetration of the latter two processes, we have scaled proton ionization cross sections by ratios appropriate for an H^0 beam injected into the same plasma, obtained by use of the HEX codes. Although this procedure is only approximate, it is sufficiently accurate for the purpose of determining feasibility of a given beam for use as a probe. A comprehensive code for a given atom species could be written, but this too would contain approximations, since many of the needed cross sections are not known.

We have studied the case of H^0-atom penetration into a plasma both because this case is of interest for CHERS and because of the existence of the HEX code. We show in Fig. 9 beam penetration for various values of Z_{eff}, mainly for C as an impurity, and, for $Z_{eff} = 1.5$ (C impurity), compare direct ionization of the fast H^0 with ionization including multistep processes. The effect of including multistep processes is to reduce the 1/e length for beam penetration by a factor of two, essentially independent of energy, for the energy range shown. The effect of the $Z_{eff} = 1.5$ (C) is to increase cross sections by a factor of 1.4.

We note that the HEX code we are using does not give exactly the penetration length we would expect for the case we checked, i.e., 750-keV H^0 energy for a $Z_{eff} = 1$ plasma (no impurities), $t_i = t_e = 10$ keV, and no excitation . The code gives a stopping cross section of 3.2×10^{-17} cm^2, while the experimental proton-ionization cross section is $2.5 \times 10^{-17} cm^2$. At this high energy we expect most the stopping to come from proton ionization (for no impurities), hence we would expect to obtain approximately the experimental cross section. We have not calculated the contribution of the low-energy tail of the electron-energy distribution. The documentation we have for the code explains that the cross section used has been "improved" at high energies by scaling to the experimental cross section. This discrepancy deserves further attention.

We have calculated the penetration of species other than H^0 into a CIT plasma. The stopping cross section (or penetration length) is estimated by taking the experimental cross section for proton ionization of the neutral atom (Fig. 8), multiplying by 2.0 to estimate the effect of multistep processes, then multiplying by 1.4 to include the effect of the C impurities

in the Z_{eff} = 1.5 plasma. The overall factor for estimating beam penetration from proton-ionization cross sections is therefore 2.8 (2.0 * 1.4). Results for penetration to the center of the plasma (100 cm) or totally through the plasma vertically (200 cm) are shown in Fig. 10. For example, the fraction of incident He^0 beam which will exit the plasma after traversing the entire 200 cm is 6×10^{-4} at 500 keV/u and 7×10^{-3} at 880 keV/u. Although this might not appear promising, it is sufficient to obtain a useful signal for a reasonable incident beam.

CHARGE-TRANSFER CALCULATION

The calculation of the charge-transfer rate between injected fast atoms in the probe beam and alpha particles in CIT requires two-electron-transfer cross sections for He^{++} at low energies, shown in Fig. 5 for various species, and an estimate of the alpha-particle energy density distribution, for which we used a spatially isotropic distribution with a total density of 3×10^{13} cm^{-3}. We have taken, for the purposes of estimating signal intensity expected, a classical velocity-distribution function,[7,8] shown in Fig. 11, which varies as v^{-3}. Measurement of the velocity-distribution function, along with its spatial and temporal characteristics, is the purpose of the diagnostic.

We can only sample alpha particles whose direction of motion allows them to exit a 5-cm-diameter port located approximately 250 cm from the center of the plasma (Fig. 2); we are thus limited to detecting alpha particles whose direction of motion is within 0.01 radian (0.57^0) relative to the axis of the injected diagnostic beam. Zero-degree observation, imposed by CIT port geometry, does not allow spatially-resolved measurement. If other port locations or an elongated port can be considered, we can extend the calculation to determine the degree of spatial resolution which can be obtained.

A curious feature of the integration over velocity (relative velocity of the target beam and alpha particles) is that the effective target length is found to be a function of relative velocity. At zero relative velocity there is no charge transfer, because, in this idealized model, the particles move parallel and at the same speed, and thus do not interact.

Let v_r be the speed of the injected diagnostic beam relative to plasma alpha particles ($v_r = (v^2 + v_b^2 - 2vv_b\cos\theta)^{1/2}$, for alpha-particle velocity v, beam velocity v_b, and angle of encounter θ), and let L be the total length of the plasma probed by the beam. Then the interaction time $t = L/v_b$ and the effective reaction length is $v_r t = L\, v_r/v_b$. We have assumed that the input and output ports are 5-cm diameter, and the distance to the center of the plasma is ~ 250 cm, which limits the beam and neutralized alpha particle divergences to ~ ± 0.01 radian. Thus the volume of velocity space probed will be approximately $(0.01)^2/4\pi$ and the relative speed $v_r = (v^2 + v_b^2 - 2\, vv_b \cos\theta)^{1/2}$ becomes just $v_r = |v - v_b|$. Hence for a velocity distribution f(v) with a total alpha-particle density n and isotropic velocity vectors, the total alpha particles neutralized in length L is

$$I_n = I_b \frac{L}{v_b} v_r \sigma(v_r) N \frac{0.0001}{4\pi} f(v) \tag{4}$$

for sufficiently small L (neglecting attenuation).

The injected neutral atom beam as well as the neutralized alpha particles will be highly attenuated by ionization in the plasma. Let $I_b(x) = I_o e^{-\lambda_1 x}$, where λ_1 is the attenuation constant of the input beam, and let $I_\alpha(x) = I_n e^{-\lambda_2(L-x)}$ be the observed intensity at the output, where λ_2

is the He^0 attenuation constant for the neutralized alpha particules. In this case,

$$I_\alpha(v) = I_o \int_0^L \int_{v_b - v_{r\,max}}^{v_b + v_{r\,max}} e^{-\lambda_1 x}\; e^{-\lambda_2 (L-x)}\; \frac{v_r}{v_b}\; \sigma(v_r)\, N\, \frac{0.0001}{4\pi}\, f(v)\, dv dx \qquad (5)$$

where v_r max is determined by the relative velocity above which the magnitude of $\sigma(v_r)$ is negligibly small. We have used the velocity which corresponds to 100 keV/u for our examples (see Fig. 5). For the special case where $\lambda_1 \simeq \lambda_2$, which is the case for an injected He^0 beam, and for a small alpha-particle velocity range about v_b, we obtain

$$\frac{I_\alpha(v)}{I_{bo}} = L\, \frac{v_r}{v_b}\, \sigma(v_r)\, N\, \frac{0.0001}{4\pi}\, f(v)\,, \qquad (6)$$

where I_{bo} is the fraction of He^0 beam exiting the plasma. (For a larger velocity range about v_b, λ_2 must be varied to account for the dependence of attenuation on the exit velocity of the neutralized alpha particles.) Since the velocity vectors are essentially parallel, we can rewrite the equation in terms of energy (including the energy-dependent beam and He^0 attenuation constants, $A_b = \lambda_1 L$ and $A_\alpha = \lambda_2 L$),

$$\frac{I_\alpha}{I_b} \cong L \sqrt{\frac{E_r}{E_b}}\; \sigma(E_r)\, N\, \frac{0.0001}{4\pi}\, f(E) * Atn(E) \qquad (7)$$

where $Atn(E) = \exp(-A_\alpha)/(A_\alpha - A_b) \times (\exp(A_\alpha - A_b) - 1)$ and where we have

replaced the velocities by energies with the same subscript. The value E_r is related to E by the square root, i.e., $E_r = (\sqrt{E} - \sqrt{E_b})^2$. Thus for an E_r range of $\pm$ 100 keV/u, the corresponding range of E is $E_b - 430 < E < E_b +$ 630 keV/u for E_b = 700 keV/u.

We have chosen a velocity distribution function for the alpha particles[7,8] (Fig. 11) that decrease as $\frac{1}{v^3}$ or $\frac{1}{E^{1.5}}$, which merges at low energy with an arbitrarily chosen low-energy (thermal) population of ~ 20-keV width, and which merges at high energy, with an alpha-particle source at 880 keV/u having a thermal width of 100 keV/u. In energy terms this function is

$$NF(E) = \frac{N}{N_o} \cdot \left(\frac{105^{1.5}}{105^{1.5} + E^{1.5}} \right) \cdot \operatorname{erf}\left(\frac{\sqrt{880} - \sqrt{E}}{100\ K} \right) \tag{8}$$

where the total alpha-particle density, N, is taken as 3×10^{13} cm^{-3}, $K = E/v^2$, E is the alpha-particle specific energy (in keV/u), and v is velocity in cm/s. The constant 105 determines the area of merging with the thermal population and N_o is the normalizing factor. The second part of the expression,

$$\operatorname{erf}\left(\frac{\sqrt{880} - \sqrt{E}}{100\ K} \right) = \int_{\infty}^{E} \exp\left(- \frac{\left(\sqrt{880} - \sqrt{E}\right)^2}{100\ K} \right) d\sqrt{E} \tag{9}$$

is the integral of the thermal distribution of the alpha particles at birth. This expression was evaluated in $\sqrt{10\ keV/u}$ steps and the results interpolated

for the calculations. Figure 11 shows this distribution as a function of alpha-particle velocity. Also shown in Fig. 11 is a distribution function which assumes an anomalous loss of fast alpha particles. This distribution is similar to the ad-hoc non-classical distribution of Ref. 8. It is produced by taking the distribution of Eqn. 8 and multiplying by the factor $(\frac{E}{880})^2$. Simulated data using these two distribution is shown in Figs. 15 and 16, which are discussed later.

Figure 12 shows the neutralized alpha-particle signal (counts/s) to be seen in a 0.01-radian cone for a probe beam of neutral He, H_2, or Li, at 700 keV/u. The relative electron-capture cross section σ_{20} for the probe beam colliding with He^{++} causes the low signal at the high- and low-energy extremes ($\pm$ 100 keV/u relative energy) while the dip in the middle is caused by the factor $|v_b - v|$ in the effective target length (related to the "reaction density" in Ref. 7). A portion of the distribution function F(E) can be determined by inverting Eq. (7),

$$N\,F(E) = \frac{I_\alpha(E)}{I_{bo}} \frac{4\pi}{0.0001} \sqrt{\frac{E_b}{E_r}} \;/\; L\sigma(E_r) \,/\, Atn(E) \qquad (10)$$

and by evaluating it at each value of E for which data can be obtained (values of $E = (\sqrt{E_b} + \sqrt{E_r})^2$ and $(\sqrt{E_b} - \sqrt{E_r})^2$).

The total signal can be calculated by use of the data in the proceeding paragraphs. A He^0 probe beam (see Fig. 12) will provide greater signal than a Li^0 or H_2^0 probe beam, because of the larger two-electron-capture cross section for He^{++} in He relative to He^{++} in Li or H_2, and because considerably more (Fig. 10) of a He^0 diagnostic beam penetrates in the CIT plasma than does a Li^0 or H_2^0 beam. However, more intense beams of Li^0 than He^0 can be produced. These factors are combined in Tables III through V, which show the total

Table III. He^0 signal exiting the plasma for a He^0 probe beam (100 mA HeH^+ accelerated current, giving an incident He^0 flux of $2x10^{16}$ particles/s).

Probe-beam Energy	He^0 attenuation factor (200-cm path length	Total He^0 signal exiting the plasma (particles/s)
900 keV/u	$8.3x10^{-3}$	$2.2x10^{7}$
800	$5.5x10^{-3}$	$1.9x10^{7}$
600	$1.7x10^{-3}$	$1.4x10^{7}$
400	$2.1x10^{-4}$	$5.8x10^{6}$

Table IV. He^0 signal exiting the plasma for a Li^0 probe beam (100 mA Li^- accelerated current, giving an incident Li^0 flux of $3x10^{17}$ particles/s).

Probe-beam energy	Li^0 attenuation factor (200-cm path length)	He^0 attenuation factor (200-cm path length	Total He^0 signal exiting the plasma (particles/s)
900keV/u	$6.6x10^{-5}$	$8.3x10^{-3}$	$6.9x10^{6}$
800	$2.5x10^{-5}$	$5.5x10^{-3}$	$4.4x10^{6}$
600	$1.5x10^{-6}$	$1.7x10^{-3}$	$5.4x10^{6}$
400	$7.3x10^{-9}$	$2.1x10^{-4}$	$4.2x10^{6}$

Table V. He^0 signal exiting the plasma for a H_2^0 probe beam (100 mA H_3^+ accelerated current, giving an incident H_2^0 flux of $2x10^{16}$ particles/s).

Probe-beam energy	H_2^0 attenuation factor (200-cm path length)	He^0 attenuation factor(200-cm path length)	Total He^0 signal exiting the plasma (particles/s)
900keV/u	$1.0x10^{-4}$	$8.3x10^{-3}$	$9.4x10^{5}$
800	$4.0x10^{-5}$	$5.5x10^{-3}$	$6.0x10^{5}$
600	$2.7x10^{-6}$	$1.7x10^{-3}$	$7.2x10^{5}$
400	$1.7x10^{-8}$	$2.1x10^{-4}$	$5.0x10^{5}$

neutralized alpha-particle signal produced within 100 keV/u relative to the probe-beam energy for He^0, Li^0, and H_2^0 probe beams. The attenuation factors for the probe beam and the neutral He^0 beam due to ionization in the plasma are taken from Fig. 10, and the incident flux for 100 mA of accelerated ion current from Table II. The signals are calculated as in Eq. 7, using a 200-cm path length. The attenuation factors shown are for the probe beam energy; however, the total signal is calculated for the full energy range of the exiting signal. The total He^0 signal exiting the target, for a He^0 probe beam produced from 100 mA of accelerated HeH^+, is of the order of $1x10^7$ particles/s. This is sufficient to obtain an acceptable number of counts, $1x10^4$, in 1 ms, so that reasonable time resolution can be obtained.

RESULTS OF CHARGE-TRANSFER CALCULATION

Beams of H_2^0 and Li^0 do not penetrate the plasma sufficiently well to probe the center of CIT; most charge transfer with a Li^0 or H_2 probe beam will take place near the entrance to CIT. A more complete calculation of the He^0 (neutralized alpha particle) signal for a probe beam other than He^0 shows that, for a beam which attenuates faster than He^0, e.g., Li^0, most of this signal comes from charge transfer which takes place near the entrance of the probe beam into the plasma (i.e., before the probe beam has significantly attenuated). This could provide crude information on the spatial distribution of alpha particles in the plasma. Figure 13 shows the signal as a function of the location of the charge transfer in the plasma, for a 700-keV Li^0 probe beam. At any He^0 exit energy, more than 40% of the signal comes from the first 10% of the plasma penetrated by the beam (curve labelled 1) while only a fraction of 1% arises from the 10% of the plasma closest to the probe-beam

exit. Thus information about the alpha-particle distribution near the edge of the plasma could be obtained by use of a Li^0 probe beam. Figure 14 shows a similar set of curves for a He^0 probe beam. The largest signal comes from the last 10% for the low-energy side of the figure while the high-energy side shows a relationship similar to the curves for a Li^0 probe beam. The reason is that the beam is attenuated less than the signal for signal energies less than the beam energy, and the reverse for signal energies greater than the beam energy. Note that with no attenuation, all the curves would be the same. These results are for slab plasma; the beam will probe somewhat further into a plasma with a parabolic density profile.

Overlapping results for several probe-beam energies can be used to determine the alpha-particle velocity distribution function over a fairly large range. Results shown in Figs. 15 and 16 are for $^3He^0$ probe-beams at 400, 500, 600, 700, 800, and 900 keV/u specific energy. Shown are the flux of neutralized alpha particles exiting the plasma in counts/s per 5-keV/u energy bin, relative to the incident beam energy $\pm$100 keV/u, for 100 mA of accelerated HeH^+. The figures include attenuation of the incident $^3He^0$ and exiting $^4He^0$ for vertical passage through a CIT plasma, and are calculated using the distribution functions shown in Fig. 11. The simulated data shown in Fig. 15 correspond to the classical distribution of Equ. 8, which varies as $\frac{1}{v^3}$ over most of its width; Fig. 16 shows data which would result from the anomalous losses assumed in the non-classical distribution. The two distribution functions are clearly distinguishable by comparison of the energy dependence of the data. A large portion of the true distribution function could be determined by inverting data such as these, using measurements at several probe-beam energies.

Two-electron capture from a He-atom probe beam by the fast alpha-particles in an ignited CIT plasma presents a feasible method for determining the energy distribution of the slowing-down alpha-particles integrated along a chord in the direction along the probe-beam path with a time resolution of the order of 1 ms. Limited information about the spatial distribution of alpha particles may be determinable through the use of a probe beam which attenuates faster than He^0. This determination might be better made with optical methods in concert with the two-electron-capture method. The same He^0 probe beam which serves as a target for two-electron capture will serve as a target for one-electron capture, and CHERS measurements could be made through a horizontal part at the same time as the two-electron-capture measurements are made through vertical ports. Limited spatially-resolved information could be obtained by using appropriate access-port geometry.

REIONIZATION AND DETECTION OF FAST He^0

The fast $^4He^0$ (neutralized alpha particles) atoms exiting the plasma can be reionized to $^4He^+$ in a gas target, or to $^4He^{++}$ in a thicker gas target or foil, with an efficiency of the order of 90% for producing He^{++}. These ions can be separated from reionized ^3He probe atoms by an energy selector; the ^4He ions will be detected with a surface-barrier or other single- particle detector, while the ^3He ions will be detected by a Faraday cup or a surface-barrier detector, depending on the intensity. The energy distribution for the reionized ^4He ions can be obtained from the energy resolution inherent in the surface-barrier detector. Energy resolution may be improved if necessary by use of a position-sensitive detector. A gas cell will be essentially transparent to the intense neutron and gamma flux emitted by the plasma, and thus unaffected, and the detectors, removed from line-of-sight of the plasma, can be well shielded.

CONCLUSION

A two-electron-capture diagnostic for fast confined alpha particles in CIT appears to be feasible. Appreciable signal will be obtained, allowing measurement of the alpha-particle velocity distribution, with a trade-off between time resolution and accelerated current. We recommend further research leading to implementation on CIT. The best probe beam consists of ground-state helium atoms, because of its good penetration into a CIT plasma and large cross section for two-electron capture. A helium-atom beam can be produced from HeH^+, sufficient to allow time- and energy-resolved measurements. The most important subject for research is production of a fast He^0 atom beam, with topics to include optimization of source performance for molecular-ion production, dissociation fraction at relevant energies, and ground-state population. The fraction of He^0 atoms in the ground state, produced by neutralization of alpha particles by two-electron capture from He, should also be measured. Research leading to development of a variable-energy (5 MeV maximum for $^4HeH^+$, or 4 MeV for $^3HeH^+$ high-current accelerator should be undertaken; consideration of the relationship between time resolution and He^0 flux in the probe beam will determine the current requirement of the accelerator. Finally, our calculations should be further refined, and relevant quantities measured where needed, especially concerning penetration of a He beam into a plasma, to bring this diagnostic into sharper quantitive focus.

REFERENCES

1. D. E. Post, S. J. Zweben, and L. R. Grisham, "Alpha-Particle Diagnostics," in proceeding of Morena School on Diagnostics, 1986 (unpublished).
2. S. J. Zweben, "Approaches to the Diagnostics of Alpha Particles in Tokamaks," Rev. Sci. Instrum. 57, 1723 (1986).
3. D. E. Post, L. R. Grisham and R. J. Fonck, "Several Atomic Physics Issues Connected with the Use of Neutral Beams in Fusion Experiments," Physica Scripta. T3, 135, (1983).
4. U. Schumacher, "Considerations for Alpha-Particle Diagnostics," Physica Scripta, 1986.
5. A. S. Schlachter and W. S. Cooper, "Proposed Neutral-Beam Diagnostics for Fast Confined Alpha Particles in a Burning Plasma," in "Production and Neutralization of Negative Ions and Beams, Fourth International Symposium, Brookhaven, NY, 1986," (edited by J. G. Alessi), AIP Conference Proceeding No. 158, pp. 727-738; see also A. S. Schlachter and W. S. Cooper in "Presentations from the Workshop on Alpha-Particle Diagnostics on CIT," presented at PPPL, 3-5 June, 1987. AA-8707-10-PPL-06.
6. Alpha-Particle Effects Workshop, Courant Institute of Mathematical Sciences, New York University, December 5-6, 1985; Presentations from the Workshop on Alpha-Particle Diagnostics on CIT, PPPL, 3-5 June 1987.
7. L. R. Grisham, D. E. Post, and D. R. Mikkelsen, "Multi-MeV Li^0 Beam as a Diagnostic for Fast Confined Alpha Particles," Nucl. Technol./Fusion 3, 121 (1983).
8. D. E. Post, D. R. Mikkelsen, R. A. Hulse, L. D. Stewart, and J. C. Weisheit, "Techniques for Measuring the Alpha-Particle Distribution in Magnetically Confined Plasmas," J. Fusion Energy, 1, 129 (1981).

9. M. Sasao and K. N. Sato, "Alpha-Particle Diagnostics with High-Energy Neutral Beams," Nagoya University, IPPJ-695, Sept. 1984; Fusion Technology 10, 236 (1986).

10. M. Sasao, K. N. Sato, Y. Nakamura and M. Wakatani, "Active Diagnostics of Magnetically Confined Alpha Particles by Pellet Injection," Nagoya University, IPPJ-757, Jan. 1986; Nuclear Fusion 27, 335 (1987).

11. L. R. Grisham, D. E. Post, and J. M. Dawson, Nucl. Technology/Fusion 4, 452 (1983); F. E. Cecil, S. J. Zweben, and S. S. Medley, Nucl. Instrum. Methods A245, 547 (1986); D. R. Slaughter, Rev. Sci. Instrum. 56, 1100 (1985).

12. R. J. Fonck, "Charge-Exchange Spectroscopy as a Plasma Diagnostic Tool," Rev. Sci. Instrum. 56, 885 (1985).

13. R. E. Olson, private communication.

14. M. B. Shah and H. B. Gilbody, "Electron Capture and $He^+(2s)$ Formation in Fast He^{2+} + H and He^+ + H Collisions," J. Phys. B 11, 121 (1978).

15. G. A. Murray, J. Stone, M. Mayo, and T. J. Morgan, "Single and Double Electron Transfer in He^{2+} + Li Collisions," Phys. Rev. A 25, 1805 (1982); R. W. McCullough, T. V. Goffe, M. B. Shah, M. Lennon, and H. B. Gilbody," Electron Capture by He^{2+} and He^+ Ions in Lithium Vapor," J. Phys. B 15, 111 (1982).

16. W. S. Cooper, "Use of the Kalman Filter in Signal Processing to Reduce Beam Requirements for Alpha-Particle Diagnostics," Rev. Sci. Instrum. 57, 1846 (1986); "Use of Optimal Estimation Theory, in Particular the Kalman Filter, in Data Analysis and Signal Processing," Rev. Sci. Instrum. 57, 1846 (1986).

17. K. H. Berkner, R. V. Pyle, J. W. Stearns, and J. C. Warren, "Single- and Double-Electron Capture by 7.2- to 181-keV $^3He^{++}$ Ions in He," Phys. Rev. 166, 44 (1968); M. B. Shah and H. B. Gilbody, "Formation of $He^+(2s)$ Metastable Ions in Passage of 10-60 keV $^3He^{2+}$ Ions through Gases," J. Phys. B 7, 256 (1974).

18. R. D. DuBois, "Ionization and Charge Transfer in He^{2+}-Rare-Gas Collisions," Phys. Rev. A33, 1595 (1986).

19. M. B. Shah and H. B. Gilbody, "Charge Transfer and Formation of Metastable $He^+(2)$ Ions in Collisions of $^3He^{2+}$ Ions with Potassium," J. Phys. B 7, 637 (1974).

20. Y. Nakai, A. Kikuchi, T. Shirai, and M. Sataka, "Data on Collisions of Helium Atoms and Ions with Atoms and Molecules," JAERI-M 84-069, April, 1984; K. Okuno, "Charge-Changing Cross Sections for Heavy-Particle Collisions in the Energy Range from 0.1 eV to 10 MeV: I. Incidence of He, Li, Be, B, and Their Ions". IPPJ-AM-9, December, 1978.

21. W. L. Nutt, R. W. McCullough, K. Brady, M. B. Shah, and H. B. Gilbody, "Electron Capture by He^{2+} Ions in Collisions with H and H_2 at Impact Energies Below 10 keV," J. Phys. B 11, 1457 (1978).

22. A. S. Schlachter, "Metastable Contamination of Fast He^0 Beams Produced from He^-," Bull. Am. Phys. Soc. 25, 698 (1980).

23. J. W. Stearns, K. H. Berkner, R. V. Pyle, B. P. Briegleb and M. L. Warren, "Dissociation Cross Sections for 0.5- to 1-MeV HeH^+ Ions in H_2, He, N_2, and Ne Gases," Phys. Rev. A4, 1960 (1971).

24. K. H. Berkner, T. J. Morgan, R. V. Pyle, and J. W. Stearns, "Collision Cross Sections of 400- to 1800-keV H_3^+ Ions in Collisions with H_2 and N_2 Gases," Phys. Rev. A8, 2870 (1973).

25. K. N. Leung (private communication).

26. A. S. Schlachter, "Formation of Negative Ions by Charge Transfer: He^- to Cl^-," in "Production and Neutralization of Negative Ions and Beams (3rd Int'l Symposium, Brookhaven, 1983)," (edited by Krsto Prelec), AIP Conference Proceedings No. 111, pp. 300-311.

27. S. Walter, K. N. Leung, and W. B. Kunkel, LBL-23298 (1987); Appl. Phys. Lett. 51, 566 (1987).

28. Conversion of Li^+ to Li^- by charge transfer has an efficiency of 5%, as reported by J. R. Mowat, E. E. Fisch, A. S. Schlachter, J. W. Stearns, and Y. K. Bae, "Equilibrium charge-state fractions of Li^-, Li^0, and Li^+ in Mg, Sr, and Cs Vapors," Phys. Rev. A31, 2893 (1985).

29. L. R. Grisham, D. E. Post, B. M. Johnson, K. W. Jones, J. Barrette, T. H. Kruse, I. Tserruya, and W. Da-Hai, "Efficiencies for Gas Neutralizers for Multi-MeV Beams of Light Negative Ions," Rev. Sci. Instrum. 53, 281 (1982).

30. D. E. Post, R. K. Janev, C. D. Boley, and R. Wieland, "Influence of Excited States on Neutral-Beam Heating," (unpublished).

31. D. S. Elliott, M. B. Shah, and H. B. Gilbody, "Ionization and Charge Transfer in Collisions of H^+ and He^+ with Potassium," J. Phys. B 19, 3277 (1986).

32. M. B. Shah and H. B. Gilbody, "Single and Double Ionization of Helium by H^+, He^{2+} and Li^{3+} Ions," J. Phys. B 18, 899 (1985).

33. M. B. Shah, D. S. Elliott, and H. B. Gilbody, "Ionization and Charge Transfer in Collisions of H^+ and He^{2+} with Lithium," J. Phys. B 18, 4245 (1985).

34. M. B. Shah and H. B. Gilbody, "Ionization of Atomic Hydrogen by 4.8 MeV C^{6+} Ions," J. Phys. B 16, L449 (1983).

35. M. B. Shah and H. B. Gilbody, "Crossed-Beam Coincidence Studies of Ionization and Electron Capture in Collisions of Multiply Charged Ions with Hydrogen Atoms," J. Phys. B 16, 4395 (1983).

36. M. B. Shah and H. B. Gilbody, "Experimental Study of the Ionization of Atomic Hydrogen by Fast Multiply Charged Ions of Carbon, Nitrogen and Oxygen," J. Phys. B 14, 2831 (1981).

37. M. B. Shah and H. B. Gilbody, "Experimental Study of the Ionization of Atomic Hydrogen by Fast H^+ and He^{2+} Ions," J. Phys. B 14, 2361 (1981).

38. M. B. Shah and H. B. Gilbody, "Ionization of H_2 by Fast Protons and Multiply Charged Ions of He, Li, C, N and O," J. Phys. B 15, 3441 (1982).

39. C.D. Boley, R.K. Janev, and D.E. Post, "Enhancement of the Neutral-Beam Stopping Cross Section in Fusion Plasmas due to Multistep Collision Processes," Phys. Rev. Lett. 52, 534 (1984).

CAPTIONS

Fig. 1 Schematic diagram of neutral-beam diagnostic methods for fast confined alpha-particles: one- and two-electron capture.

Fig. 2 Vertical-access geometry assumed for CIT.

Fig. 3. Cross sections (in cm^2) for single-electron capture of $He^{++} + H^0$ to form $He^+(n)$, estimated from calculations by R. E. Olson. Shown for comparison (dashed line) are cross sections for two-electron capture of He^{++} to form He^0.

Fig. 4. Energy-level diagram of He^+, showing transition wavelengths in Å.

Fig. 5. Cross sections for capture of two electrons by He^{++} in collision with various atoms and molecules.

Fig. 6. Charge-state fractions as a function of target thickness for 5-MeV HeH^+ in H_2. The yield of He^0 is about 3%.

Fig. 7. Charge-state fractions as a function of target thickness for 3-MeV H_3^+ in H_2. The yield of H_2^0 is about 4%. (Note the thinner optimum target than for the system in Fig. 6).

Fig. 8. Cross section for ionization of atoms and molecules by protons (or, in some cases, by electrons at the same velocity as a proton). A good candidate for penetration into a plasma will have a small cross section.

Fig. 9. Calculation of penetration of H^0 atoms into a plasma with Z_{eff} shown (for C or Fe impurity, indicated in parentheses). The 1/e length is shown for a CIT plasma, i.e., a D-T plasma of ion density $5 \times 10^{14} cm^{-3}$, with $T_i = T_e = 10$ keV. The length was calculated using the HEX code, including multistep processes, except for the top line, for which multistep (excitation) processes were not included.

Fig. 10. Calculation of surviving fraction of atoms or molecules after traversing to the center (100 cm) or totally across (200 cm) a CIT plasma in a vertical plane. Plasma parameters assumed are density 5×10^{14} cm^{-3}, $Z_{eff} = 1.5$, with carbon as the impurity, $T_i = T_e = 10$ keV.

Fig. 11 Classical and non-classical alpha-particle velocity distribution assumed for calculations of charge transfer.

Fig. 12 Signal for 700-keV/u He^0, H_2^0, and Li^0 probe beams using the classical distribution function.

Fig. 13 Signal as a function of location of charge transfer in the plasma (measured from entrance of probe beam) for 700-keV/u Li^0 probe beam. Most of the He^0 signal observed arises from charge transfer near the edge (probe-beam entrance) of the plasma, because of rapid beam Li^0 attenuation compared to He^0 attenuation in the plasma. The small number 1 indicates signal arising from charge transfer in the first 10% of the path through the plasma, 2 indicates signal from the second 10% of the plasma, and so on.

Fig. 14 Same as Fig. 13, for 700-keV/u He^0 probe beam. The small numbers have the same meaning as in Fig. 13. Notice, however, that the curves are inverted for the low-energy peak (see text).

Fig. 15 $^4He^0$ signal (counts/s) for a $^3He^0$ probe beam produced from 100 mA $^3HeH^+$ beam, shown as a function of $^4He^0$ (neutralized alpha particle) energy, for $^3He^0$ probe-beam energies of 400, 500, 600, 700, 800, and 900 keV/u and the classical distribution function of Eqn. 8. The signal shown is counts/s per 5-keV/u energy bin, relative to the incident beam energy $\pm$100 keV/u. Attenuation of beam and signal is included.

Fig. 16 Same as Fig. 15, for the non-classical alpha-particle distribution.

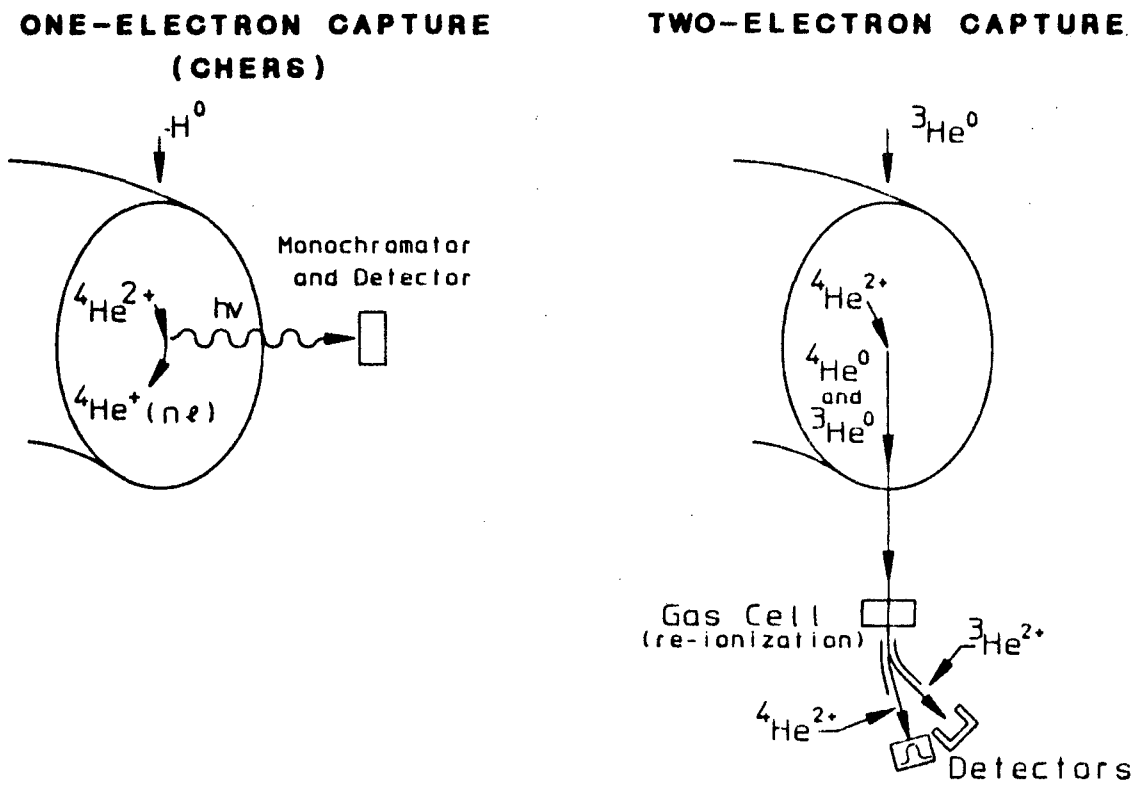

XBL 8711-4655

Fig. 1

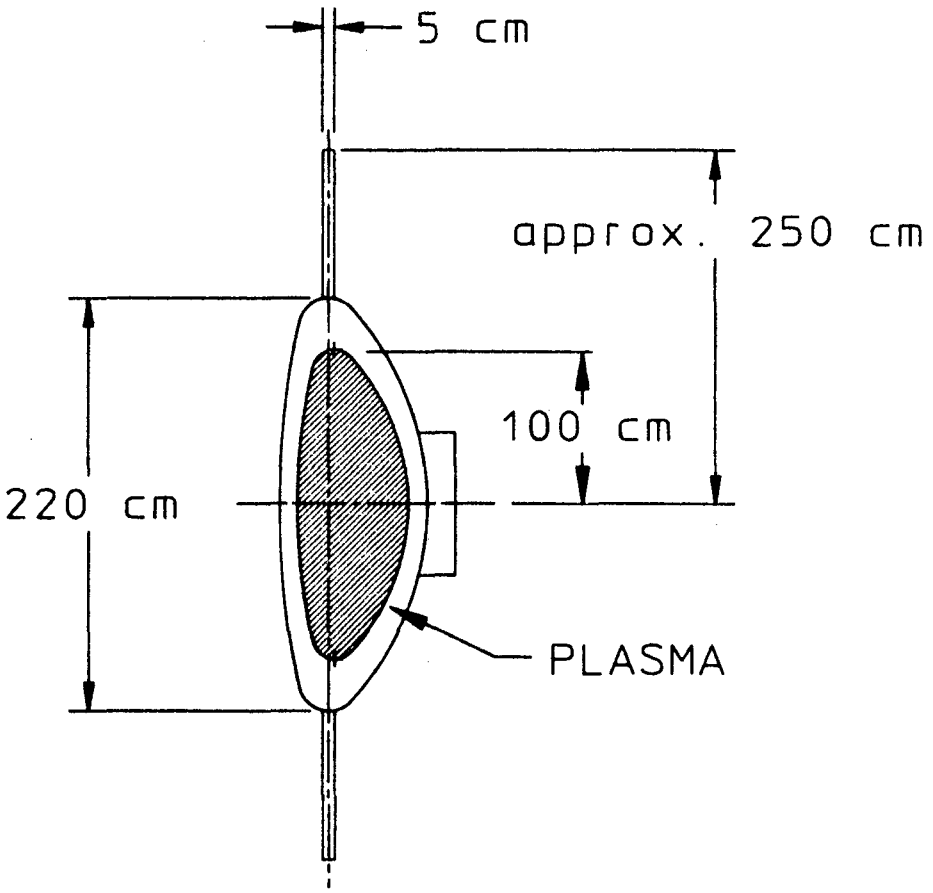

XBL 8711-4656

Fig. 2

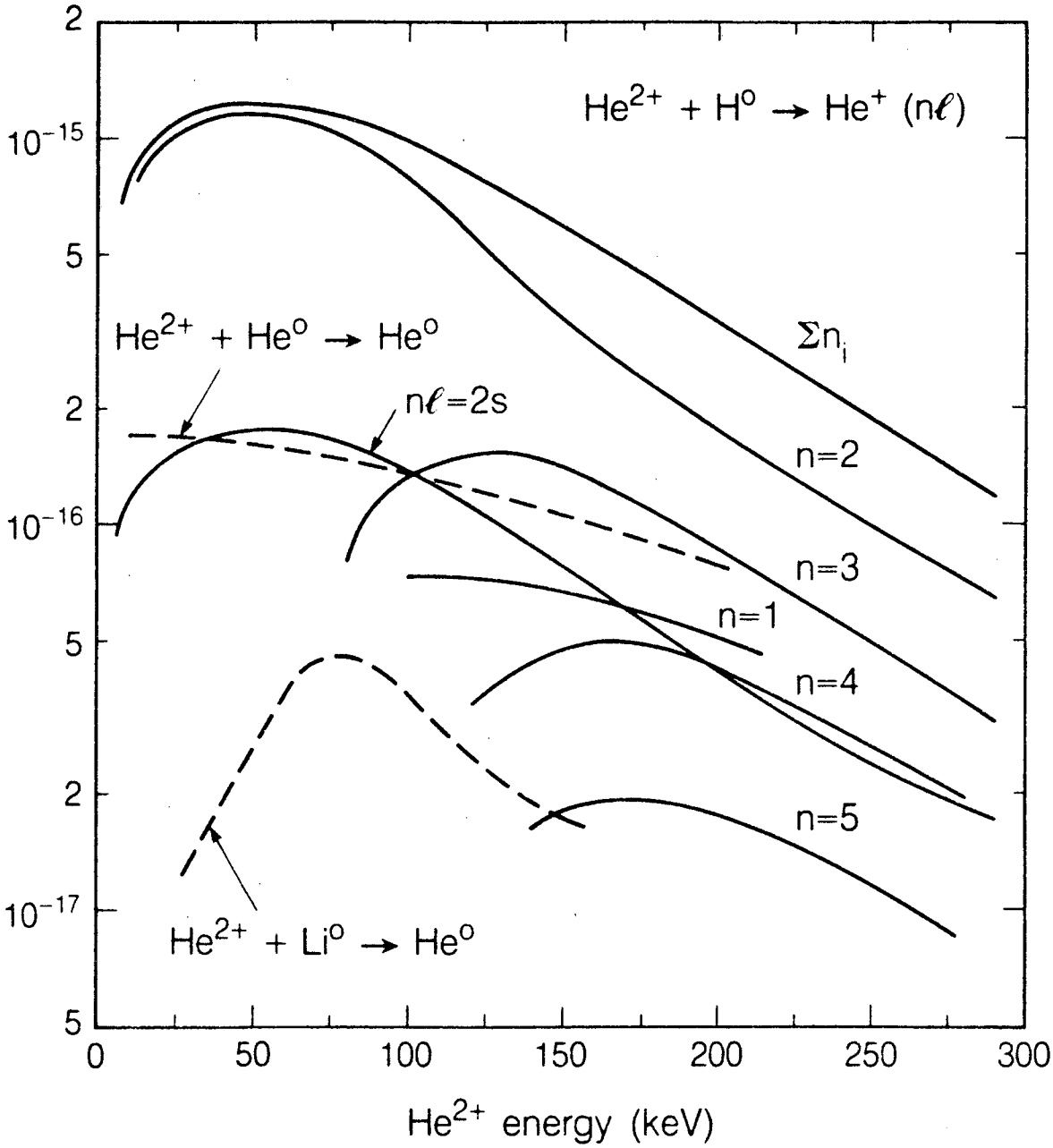

XBL 8610-9943

Fig. 3

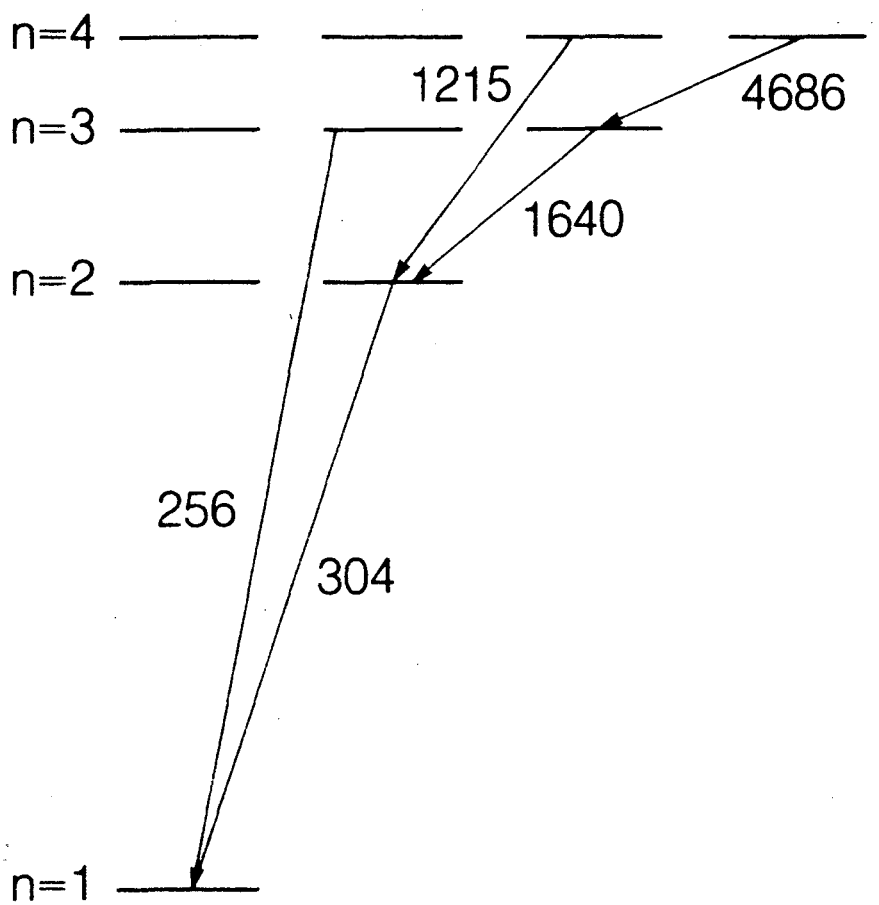

XBL 8610-9944

Fig. 4

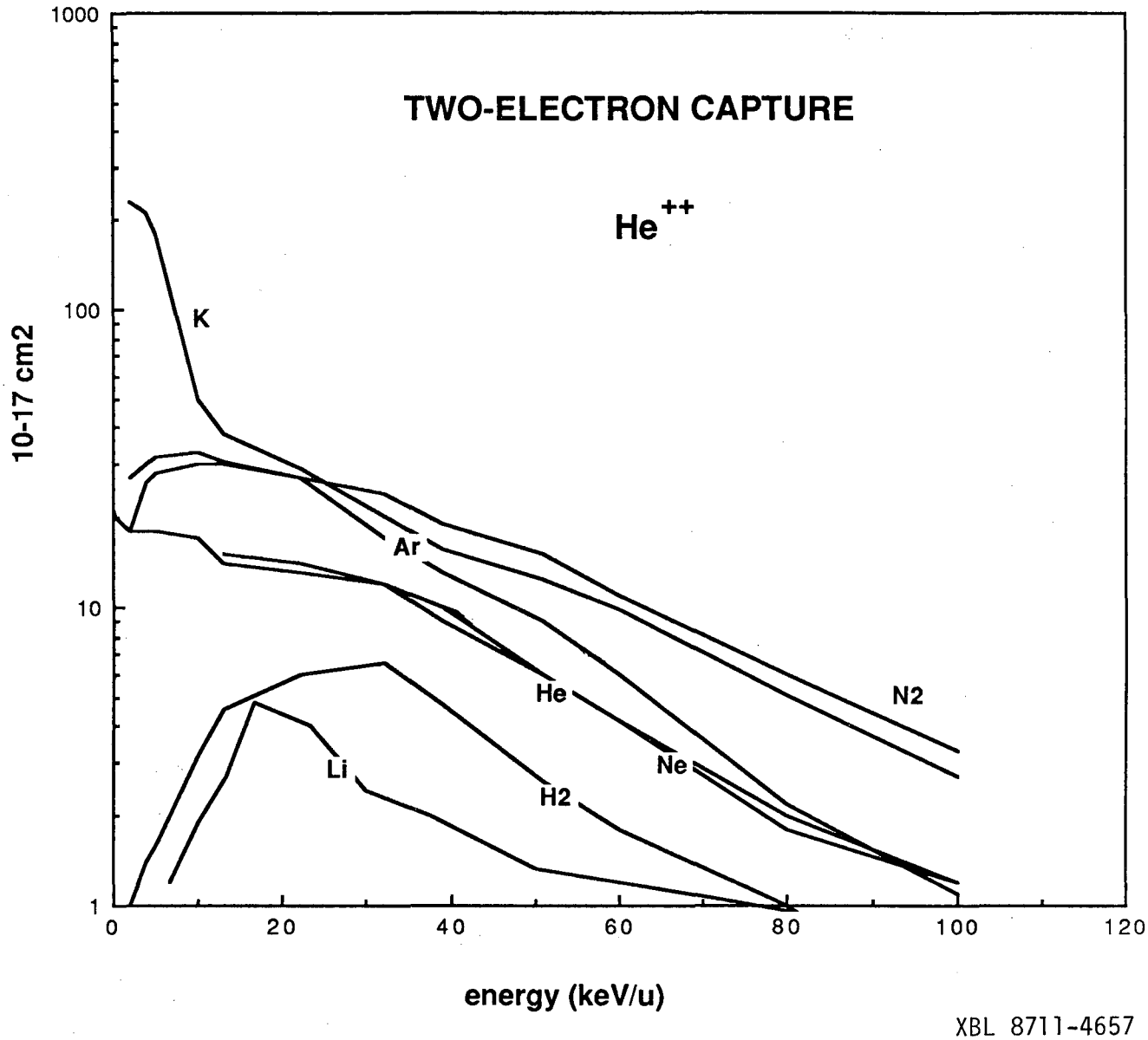

XBL 8711-4657

Fig. 5

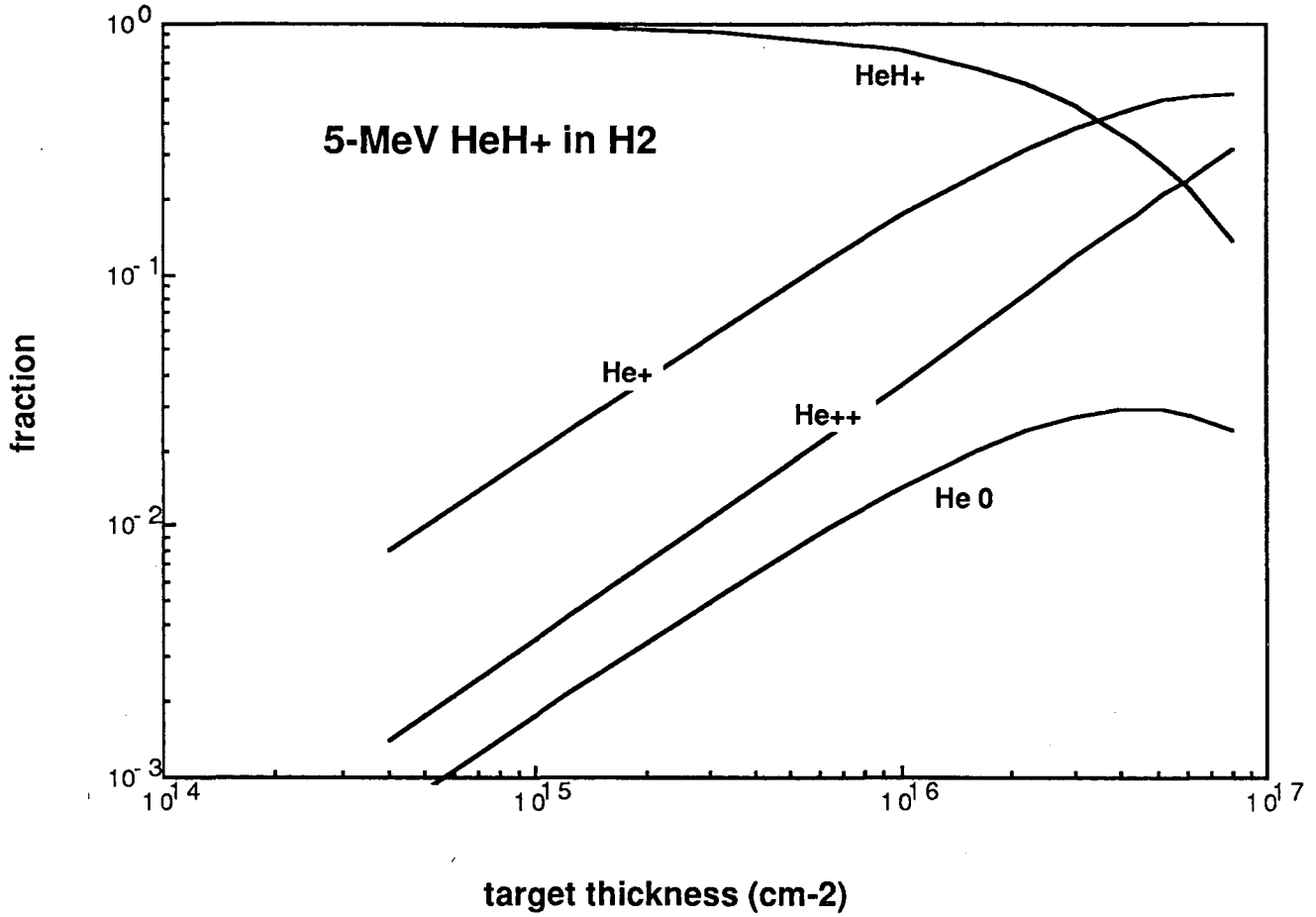

XBL 8711-4658

Fig. 6

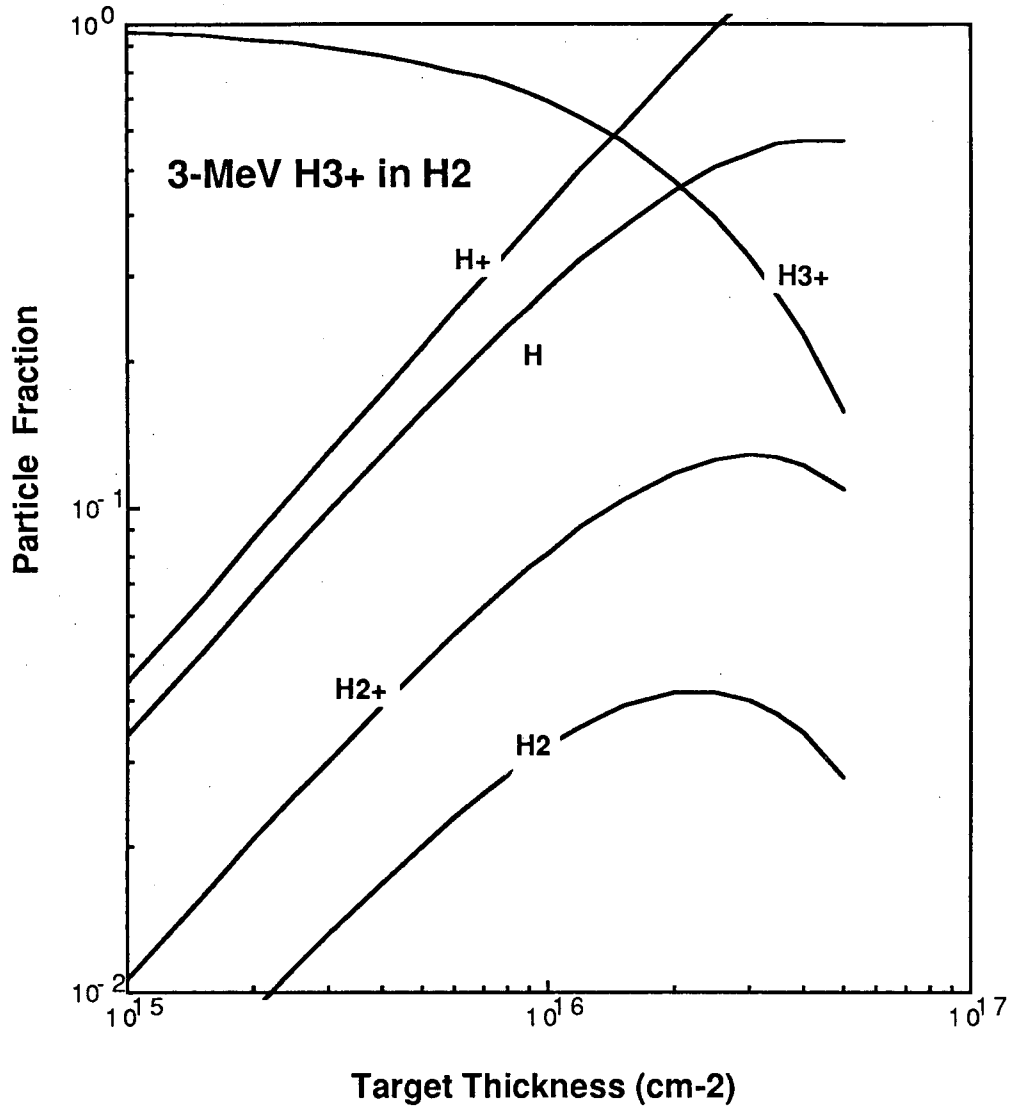

XBL 8711-4659

Fig. 7

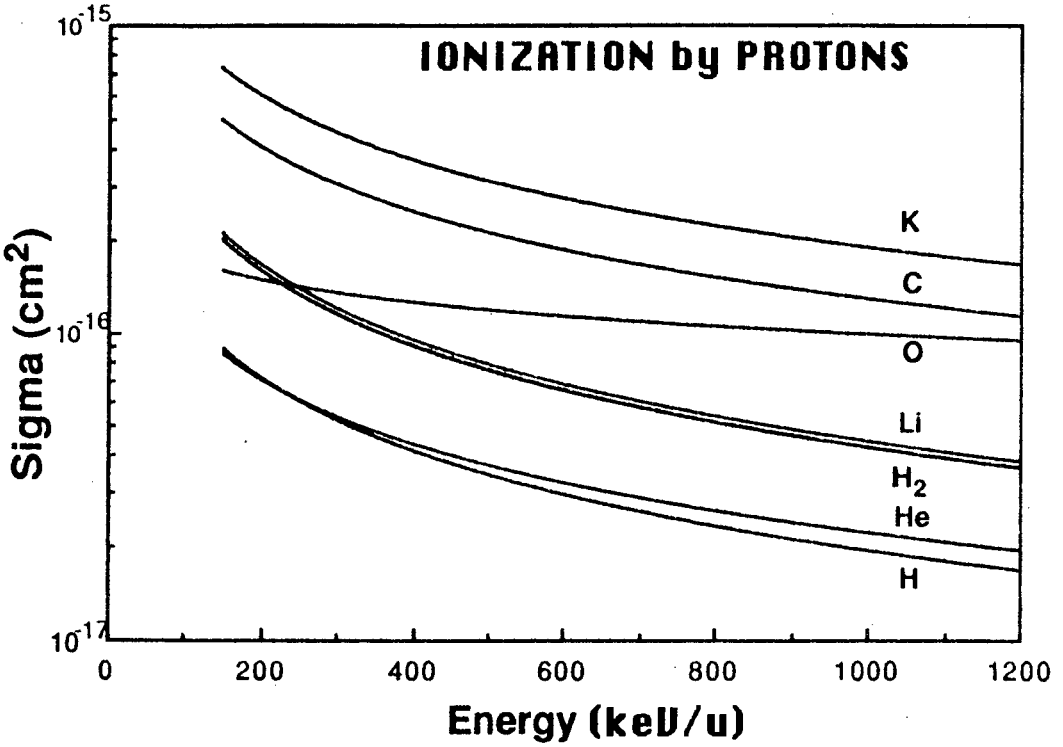

XBL 8711-4660

Fig. 8

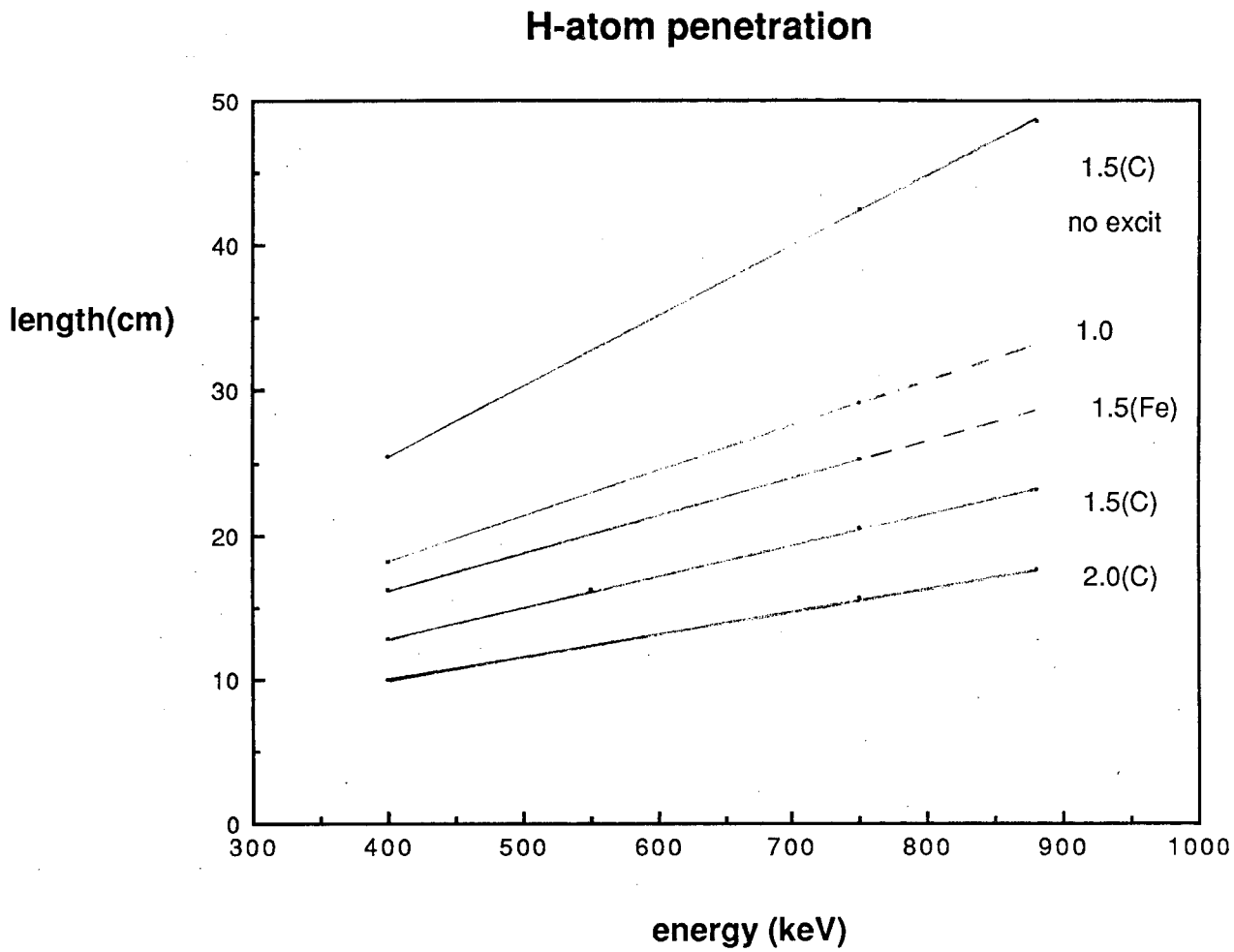
H-atom penetration
length(cm)
50
40
30
20
10
0
300
400
500
600
700
800
900
1000
energy (keV)
1.5(C)
no excit
1.0
1.5(Fe)
1.5(C)
2.0(C)
XBL 8711-4661

Fig. 9

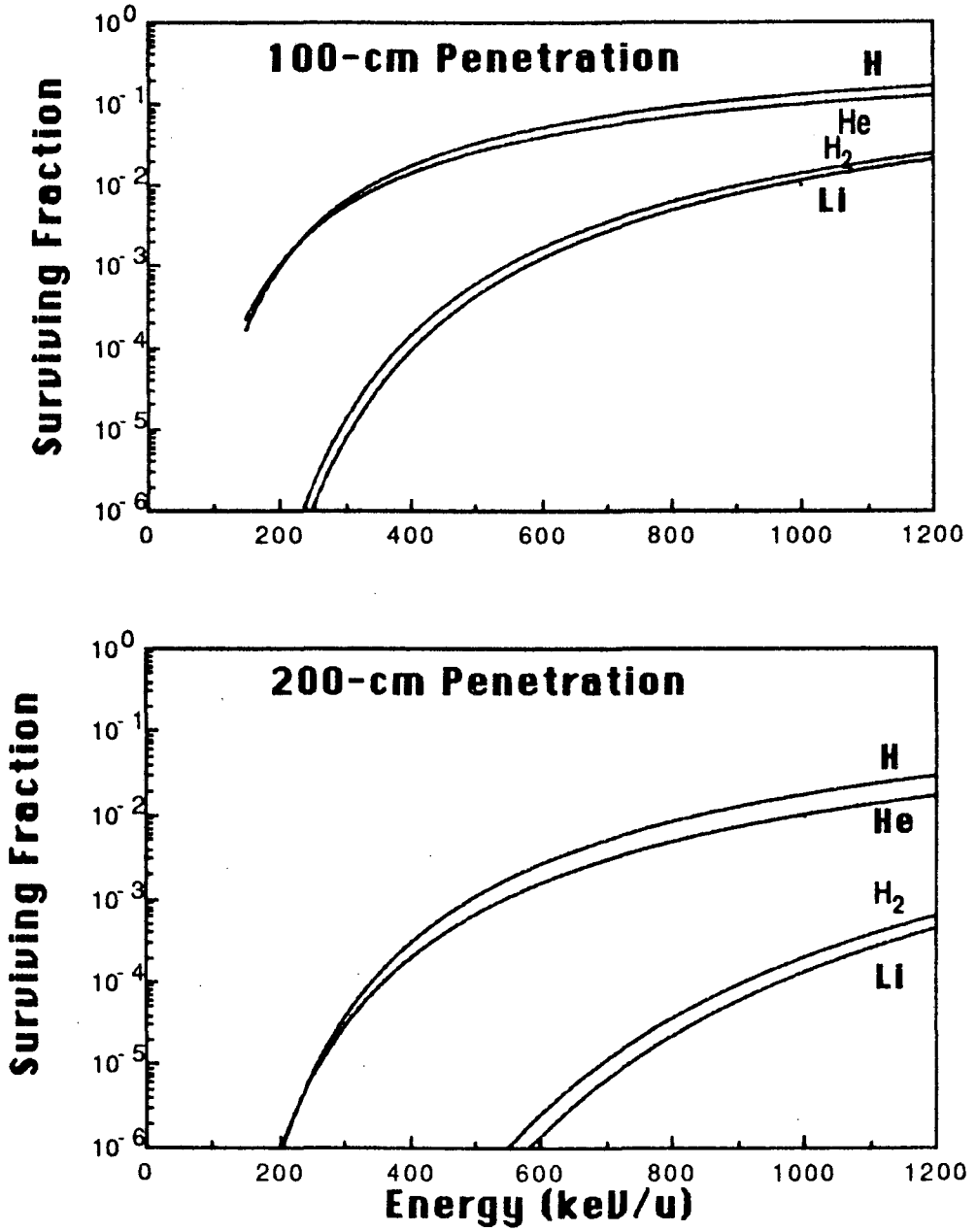
100-cm Penetration
H
He
H_2
LI
Surviving Fraction
200-cm Penetration
H
He
H_2
LI
Surviving Fraction
Energy (keV/u)
XBL 8711-4662

Fig. 10

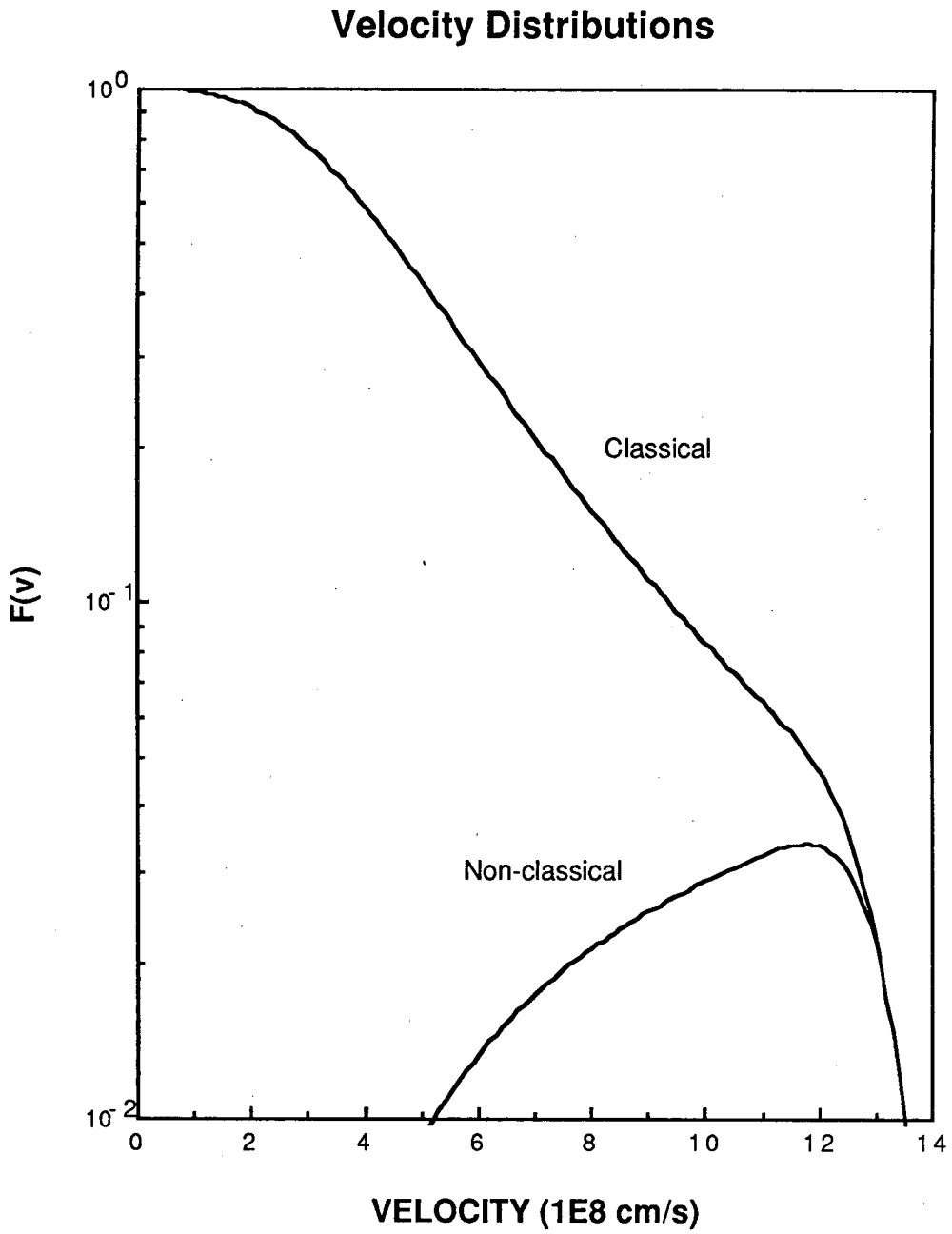

XBL 8711-4663

Fig. 11

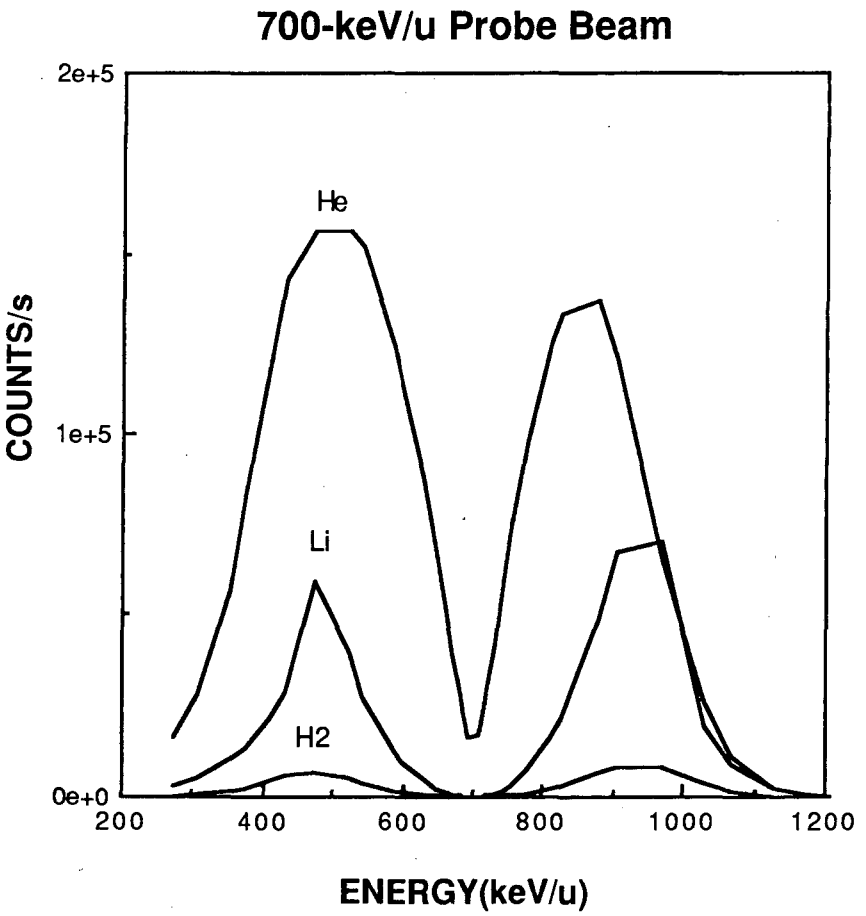

XBL 8711-4664

Fig. 12

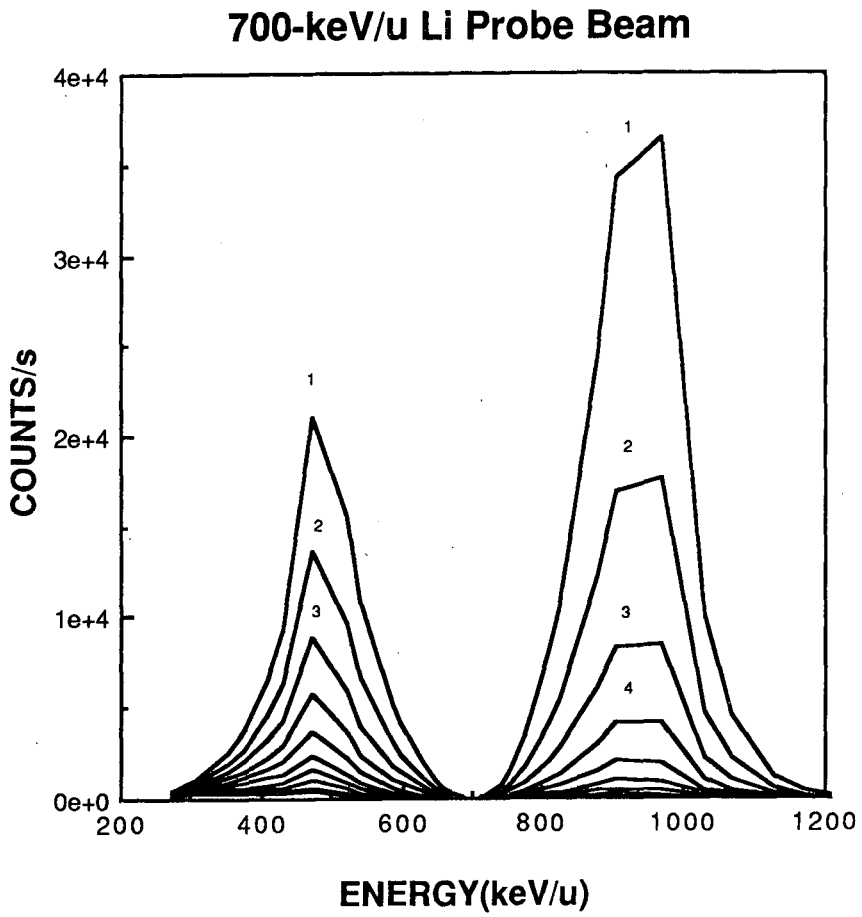

XBL 8711-4665

Fig. 13

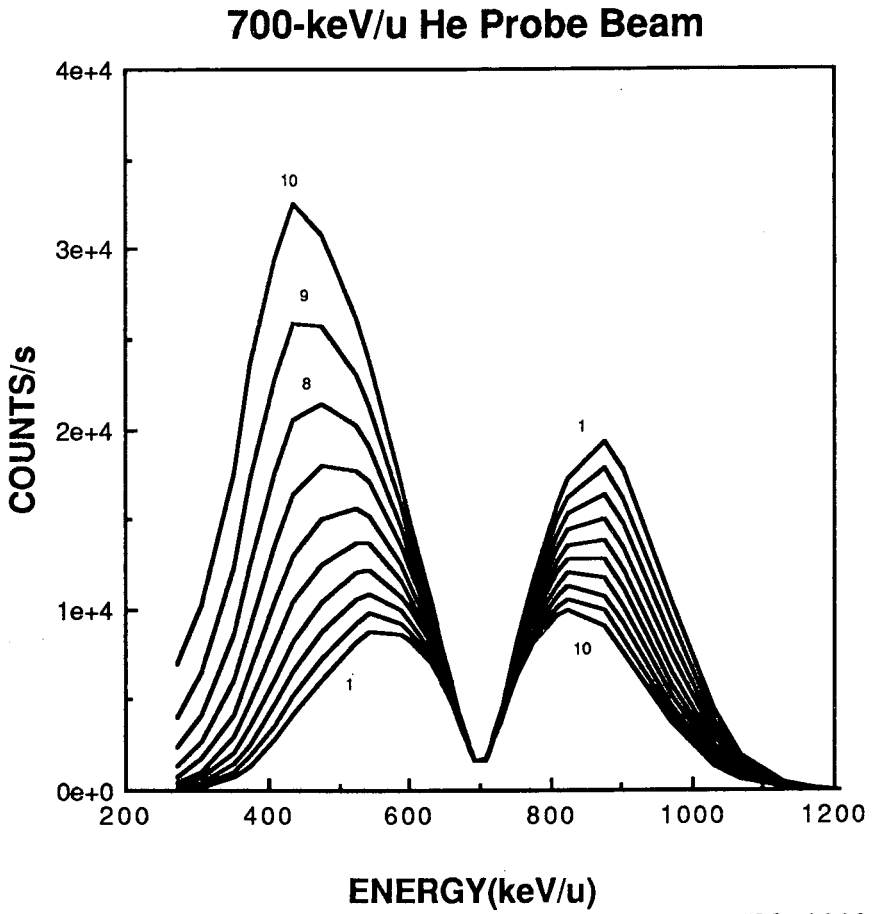

XBL 8711-4666

Fig. 14

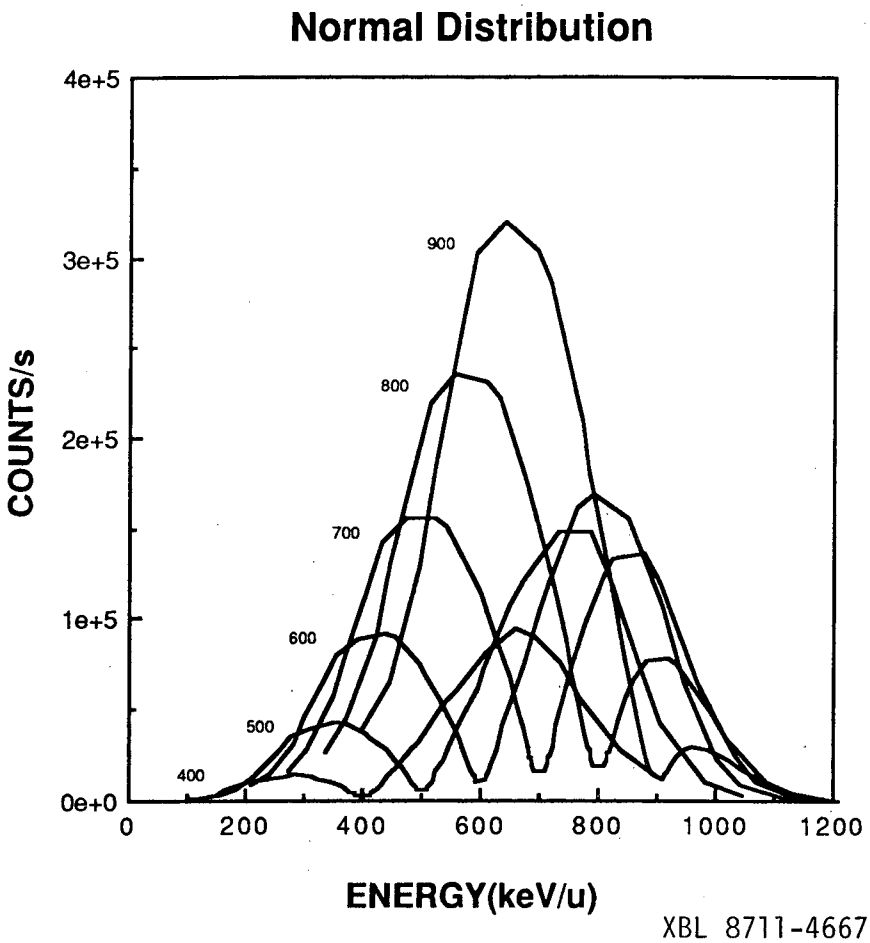
Normal Distribution
4e+5
3e+5
2e+5
1e+5
0e+0
COUNTS/s
0
200
400
600
800
1000
1200
ENERGY(keV/u)
900
800
700
600
500
400
XBL 8711-4667

Fig. 15

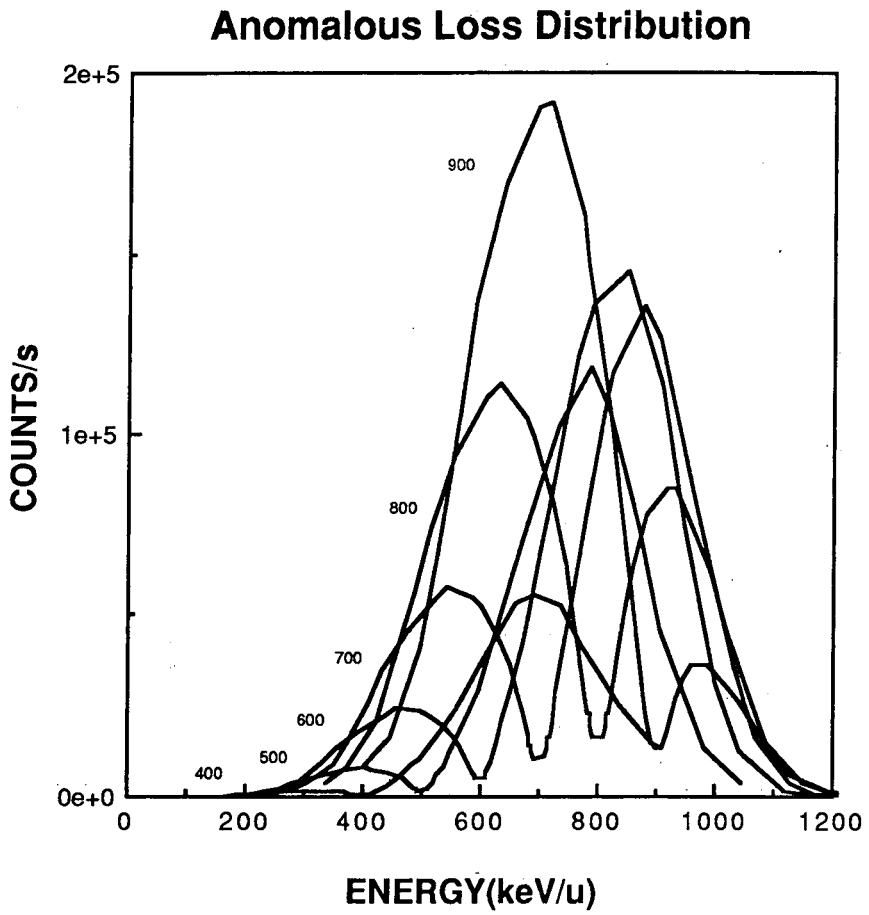
Anomalous Loss Distribution
2e+5
1e+5
0e+0
COUNTS/s
900
800
700
600
500
400
0
200
400
600
800
1000
1200
ENERGY(keV/u)
XBL 8711-4668

Fig. 16

LAWRENCE BERKELEY LABORATORY
TECHNICAL INFORMATION DEPARTMENT
UNIVERSITY OF CALIFORNIA
BERKELEY, CALIFORNIA 94720